Carbon Consumption, the Carbon-Based Ecosystem, and Output*

Cristian Figueroa†, Rodrigo Harrison‡, Roger Lagunoff§, and Mario J. Miranda¶

April 12, 2020

Abstract

This paper studies the effects of the carbon-based ecosystem on a country's output. We propose and estimate a dynamic game production model in which a country's ecosystem, as measured by its reservoir of carbon in land biomass and soils, is a productive input. Non-monotone land sink absorption of atmospheric carbon is the primary feedback channel from increased GHG concentrations. In equilibrium, a country's land carbon policy accounts for its direct effects on the ecosystem and on diminished land sink as GHG concentrations increase. We first estimate land sink absorption rates and the output elasticities of land use and the land carbon ecosystem for 152 countries. Calibrating the model to these estimates, we simulate the model to 2100 under four standard Representative Concentration Pathway scenarios. In the simulation, all countries experience higher average annual GDP growth under lower GHG concentration scenarios. However, the growth differentials between high and low scenarios are starkest for more developed countries. When compared to a "counterfactual" constant sink model, the decline of land carbon absorption makes little difference in low concentration scenarios, but decreases global GDP growth by around 1.3% per year over the next 80 years in the highest scenario. Again, the differences are most pronounced in developed countries.

JEL Codes: C54, C72, Q24, Q54, Q57
Key words: Carbon-based ecosystem, land stocks, land carbon sinks, GHG concentrations, equilibrium land use, policy-adjusted elasticity, Representative Concentration Pathways.

---

*Authors are listed alphabetically. We thank Hans Schlechter and Rodrigo Yáñez for valuable research assistance.
†Boston College, cafigue3@uc.cl.
‡Universidad Adolfo Ibañez, rodrigo.harrison@gmail.com.
§Georgetown University, lagunofr@georgetown.edu (corresponding author).
¶The Ohio State University, miranda.4@osu.edu.

1 Introduction

The carbon-based ecosystem can be viewed as a type of "capital stock" that enters directly as a productive input. Comprising the reservoir of un-extracted carbon contained in land biomass and soils, this ecosystem adds value to a country's economy in any number of ways. It preserves soil nutrients, prevents erosion, flooding, and habitat loss, it acts as a filtration system for human and animal waste, and serves as a natural climate stabilizer (IPCC, 2014; Mcalpine and Wotton, 2009).

This paper studies the effects of changes in the carbon-based ecosystem on a country's output. We propose and estimate a dynamic game model of economic growth in which fossil fuel consumption, capital-emissions intensity, land carbon use, and this ecosystem are all inputs in the production technology. The estimated parameters are then used simulate time paths of land carbon stocks and GDP across 152 countries to the end of the century.

The model features a carbon feedback mechanism whereby increased land use and greenhouse gases (GHG) concentrations from fossil fuels can deplete a country's carbon-based ecosystem. The particular channel through which this occurs is land sink absorption. Land sink absorption, the ability of land biomass to absorb carbon from the atmosphere, arises from a subtle combination of plant photosynthesis and respiration and ground absorption of carbon. The process is not negligible. The world's stock of carbon biomass, both above and below ground, in 2010 was approximately 344 GtC (FAO, 2015; Zomer et al., 2016). The land sink flow for 2011 constituted around 0.8% of the 2010 stock, excluding anthropogenic responses (Le Quere et al., 2018). All else equal, greater absorption capacity can increase the terrestrial stock and reduce atmospheric GHGs. Thus, a land sink with greater absorption capacity helps sustain the ecosystem and mitigate the effects of climate change.

The absorption capacity of sinks, however, depends on the existing concentration of atmospheric GHGs. A number of studies indicate that increases in atmospheric GHGs initially increases but eventually decreases the reabsorption rates of carbon into plant and soils (Hikosaka et al., 2006; Thomson et al., 2008; Fernandez-Martinez et al., 2017; Raupach et al., 2014; Xu, 2015; Feng et al., 2015; Zheng et al., 2018; Hubau et al., 2020). At some point, high enough concentrations hinder the capacity of the terrestrial ecosystem to absorb GHGs from the atmosphere. In the extreme, sinks can turn negative: respiration and decomposition outweigh absorption and photosynthesis.[1]

[1]Recent droughts and beetle infestation related to droughts have, for instance, resulted in the

Our study therefore integrates a non-monotone land sink function into a dynamic game model of land use by each country. Land use encompasses a wide array of activities, including agriculture, forestry, freshwater fisheries, and urban development. Globally, land use affects GHG concentrations and these concentrations, in turn, alter terrestrial carbon sinks of all countries.

To analyze land use in the dynamic game, we characterize the *Markov Perfect equilibria (MPE) in land use policies*. A MPE land use policy is a state-contingent combination of land use and atmospheric removals (from replanting, reseeding, etc) for each country that maximizes the discounted dynamic payoff of its representative consumer after each state, given land use policies of other countries. Externalities arise because countries do not internalize the effects of their decisions on other countries' local ecosystems. Nevertheless, preserving the ecosystem is desirable to some extent because it has direct value as an input and indirect value in smoothing inter-temporal consumption.

Equilibrium land policies are shown to exist and are characterized in closed form. In equilibrium, net emissions (emissions minus removals) increase in land carbon stock and in land sink. They decrease in the output elasticity of the ecosystem and in the discount factor.

Using data on carbon stocks from the Food and Agriculture Organization of the United Nations (FAO, 2019) and land sink data from 2018 Global Carbon Project, we estimate the land sink and production parameters for 152 countries covering the time period 1990-2015. Calibrating the model to these estimates, we then simulate time paths of land carbon stocks and GDP to the end of the century.

The estimated coefficients of the sink absorption function are statistically significant and consistent with an "inverted-U-shaped" relationship between GHG concentrations and land sink rates, as indicated by the cited studies. This diminished capacity of land sink has implications for GDP since land carbon enters production both directly as an input and indirectly via the country's land use policy.

The key production parameter is the *policy-adjusted output elasticity of land carbon*. It quantifies the effect of a percentage increase in the country's land carbon stock on GDP after adjusting for equilibrium land use. The policy-adjusted elasticity determines the *net* effects from both anthropogenic and non-anthropogenic changes in the ecosystem.

The assumption that countries in the sample adopt equilibrium land use policies

forests of six states in the U.S., Arizona, Colorado, Montana, Nevada, Utah, and Wyoming, turning into sources, rather than sinks, for emissions (Mooney and Murphy, 2019).

is essential for identifying the policy-adjusted output elasticity. Country data does not distinguish exogenous land sinks from endogenous behavior. Nor does it distinguish between emissions and removals. Exogenous and endogenous sources and sinks cannot be disentangled. Thus, in the absence of an equilibrium model of land use, the policy-adjusted elasticity is not identified in the production function.

Using the equilibrium land policy to pin down elasticities, we obtain estimates for four clusters of countries. Each country cluster is grouped according to the United Nations Human Development Index (HDI). A country is categorized as either High, Medium High, Medium Low, or Low development. As a robustness check, we also obtain estimates for alternative specifications of the model and for alternative clusterings based geography, emissions, forestry stock, or GDP.

Estimated policy-adjusted elasticities are positive and statistically significant over the entire sample. They are also positive and significant in the High and Medium High Development country clusters. The measured effects are sizable. Applied to the U.S., for instance, the observed increase in U.S. land carbon stock from 2010 to 2015 would, after controlling for changes in other inputs and total factor productivity (TFP), account for around 350 billion USD. The effects are higher in China, where the observed increase in its land stock from 2010-25 accounts for roughly 3.8 trillion USD.

The estimated policy adjusted elasticities for Low and Medium Low development countries are positive but not statistically different from zero, though the overall model fit is high. In those countries the relation between the country's ecosystem and its GDP is more tenuous over the time period in the data.

We incorporate the model-generated land use policies with estimated production and land sink parameters to simulate dynamic paths of land stocks, land sink absorption rates, and GDP for each HDI country cluster from 2020 to the end of the century. Simulations are run for each of the standard four Representative Concentration Pathway (RCP) scenarios formulated for the Intergovernmental Panel on Climate Change Fifth Assessment (IPCC, 2014). Each RCP is based on distinct scenarios for growth in fossil fuel and energy consumption, population, land emissions, mitigation investments, and climate policy (van Vuuren et al., 2011). The RCPs are labeled according to their projected levels radiative forcing ($+2.6, +4.5, +6.0, and +8.5 W/m^2$) achieved at the end of the century, relative to pre-industrial levels. Low GHG concentration scenarios incorporate assumptions on improvements in mitigation technology and successful policy coordination. High GHG concentration scenarios assume such improvements are minimal.

The resulting forecasts show all countries experiencing higher average annual

GDP growth under lower concentration scenarios. The lowest GHG concentration scenario, RCP 2.6, shows current trends in GDP growth continuing for all HDI clusters. Growth slows under high concentration scenarios. The two highest concentration scenarios exhibit a peak-and-decline pattern. In RCP 8.5, the worst case scenario, global GDP peaks around 2060, and declines thereafter.

GDP losses from high GHG concentrations are proportionately larger for developed rather than developing countries. It appears that highly specialized economies exhibit greater fragility (in GDP) to changes in the ecosystem.

A number of studies show that low rather than high development countries are more vulnerable to climate change and to ecological damage more generally. Althor, Watson, and Fuller (2016) develop indices relating to a country's vulnerability to climate change. Indices of sensitivity to land use are analyzed by Canadell et al. (2007), Thomson et al. (2008), Ito et al. (2008), Power (2010), Zomer et al. (2016), FAO (2015), and Narayan et al. (2017).

Our finding here is not necessarily at odds with these studies, since it applies only to measured GDP. We show, in fact, that developing countries experience greater deterioration of land carbon under high concentration of GHGs even as these countries fare relatively well in measured GDP. In other words, high concentrations scenarios may make developing countries both more vulnerable *and* more immune to GDP losses over the next half century.

We also compare our simulation model under the diminishing/declining land sink to a counterfactual, constant sink model. In the latter, the absorption rate is held fixed at its historical average. While there is virtually no difference between the "active" and the "constant" sink in the lowest RCP simulation, the differences are sizable and increasing in the larger concentration scenarios. Relative to the constant sink, the active land sink lowers global GDP by 8% in RCP 4.5, 19% in RCP 6.0, and 64% in RCP 8.5 by the end of the century. Under RCP 8.5, the diminishing land sink decreases global GDP growth by around 1.3% per year over the next 80 years in the highest scenario. The differences are greatest in the medium high development countries where sensitivity to declines in carbon stock is highest.

In general, apportioning the climate damage from specific channels has proved difficult. Tol (2009) distinguishes between an "enumerative" and "statistical" approaches. The enumerative approach evaluates and aggregates estimates from physical and natural sciences (e.g., estimates of coastal land loss) using market prices.[2]

[2]See Tol (2009) and Nordhaus and Moffat (2017) for surveys of empirical studies of climate damage.

Statistical studies use cross-sectional variation in output and climate within a country to estimate effects that are then extrapolated across time.

Integrated assessment models (IAMs) traditionally adopted a statistical approach. They analyzed large scale effects of GHG emissions on economic outcomes by combining elements of climate science with an economic growth model.[3] Recent IAMs have gravitated toward enumerative approaches, accounting for many of the GHG altering biogeochemical processes in great detail. Several efforts have been made to improve the accuracy of the models (Meinshausen, Raper, and Wigley, 2011). However, the way in which these processes are modeled differ across IAMs (Calel and Stainforth, 2017), leading to different climate change forecasts and subsequent policy recommendations.

The present study is a hybrid of various approaches. It exploits variation in land carbon stocks and output. It also focuses on one specific process and develops a simplified but tractable method of evaluating its effects in a dynamic equilibrium choice model. Other potential harms are omitted from the analysis, which suggests that the losses reported here may be lower bounds on harms not already included in the RCP scenarios.

The paper is organized as follows. Section 2 develops the model, starting with a rudimentary model of the carbon cycle together with a dynamic model of equilibrium carbon policy. This includes a description of country-specific production processes that incorporate the carbon-based inputs described above. The structural equations and identification strategy are described in Section 3. Section 4 describes the data and the estimation results. Section 5 describes the simulation procedure, the use of RCP projections and land sink absorption estimates, and the results. A summary discussion in Section 6 concludes the paper. The Appendix contains proofs, further documentation, and a full description of the algorithms used to estimate and simulate the model.

2 A Dynamic Model of Carbon Consumption

This section presents a discrete time, infinite horizon dynamic game model of carbon consumption among n countries. Each country consumes carbon in the form of fossil

[3]Recent economic studies and integrated assessment models of this type include Dell, Jones, and Olken (2012); Golosov et al. (2014); Acemoglu et al. (2012); Cai, Judd, and Lontzek (2012); IPCC (2014); Nordhaus (2014, 2018); Burke, Hsiang, and Miguel (2015); Cai et al. (2015); Hsiang et al. (2017); Deryugina and Hsiang (2017); Hassler and Krusell (2018), and many others.

fuels and land use. The model focuses on a specific feedback channels from carbon emissions to land carbon stocks and land use. The feedback channels determine the evolution of the terrestrial carbon ecosystem over time.

The model is less detailed than most IAMs. It does not contain a highly detailed and disaggregated energy sector. Energy pricing and market outcomes are exogenous. Land use, however, is endogenously influenced by rational, forward looking authorities who are cognizant of the dynamic trade offs between current and future consumption.

At each decision date $t = 0, 1, 2, \ldots$, a country faces a dynamic trade-off between the positive effects of carbon consumption and the negative effects on its terrestrial ecosystem from that consumption. All decisions take place in a rudimentary model of the carbon cycle. The next subsection lays out the carbon accounting and then proceeds with the economic model.

2.1 Global Carbon Accounting

In standard methods of carbon accounting, the global stock of carbon is constant. The carbon cycle shifts various portions of the stock to various reservoirs. This, in turn, defines a mass balance equation at each date t, represented as a sum of fluxes, i.e., net changes land, atmospheric, marine, and fossil fuel carbon stocks, the sum of which zeroes out in the aggregate:

Many of the regulating forces that determine the mass balance are non-anthropogenic, including plant photosynthesis and respiration and carbon diffusion between oceans and atmosphere. However, these flows are also influenced by human activities. Both anthropogenic and non-anthropogenic forces account for flows into and out of terrestrial or land carbon biomass. Formally:

$$\omega_t^{lan} = \omega_{t-1}^{lan} - (c_t^{lan} - r_t^{lan}) + s_t^{lan}, \tag{1}$$

where ω_t^{lan} denotes the land carbon stock at t. It comprises the terrestrial stock of carbon found in plants, animals, leaf litter, and organic matter in soils. The anthropogenic sources are c_t^{lan} and r_t^{lan}. Here, c_t^{lan} is the consumption/emissions into the atmosphere from the land stock, while r_t^{lan} is the removal from the atmosphere and into land carbon stocks at date t. Land consumption constitutes activities such as deforestation, agricultural harvests, animal husbandry, and natural resource extraction. Removals (from the atmosphere) include reforestation, replanting, and preservation. Logically, the emissions and removals activities must be distinguished since removals are akin to an investment in future capacity and so it does not directly

enter into current output of any country. The difference $c_t^{lan} - r_t^{lan}$ accounts for land use change and forestry (LUCF).[4]

The term s_t^{lan} is the global *land sink* representing non-anthropogenic removals of carbon from the atmosphere. It comprises the total net carbon absorption by unmanaged biomass due to photosynthesis and other factors. By definition it excludes LUCF.

Land sink is affected by a "wide range of environmental changes which include climate change (water and temperature), disease outbreaks, added nutrients (CO2 and nitrates), ... and re-growth of vegetation in natural (unmanaged) land that is not included under the UNFCCC reporting guidelines for LULUCF." (Ito et al. (2008), p.3292). The definition accounts for most of the feedback effects of greenhouse gases that are not directly associated with contemporaneous human activity.

Both land use and fossil fuel consumption produce carbon flows from terrestrial carbon stocks and fossil fuel reserves into atmosphere. At the same time, atmospheric greenhouse gases flow back to land stocks via a land sink absorption mechanism.

Recent results from Hikosaka et al. (2006) Raupach et al. (2014), Xu (2015), Zheng et al. (2018), and Hubau et al. (2020) indicate an inverted-U relationship between atmospheric greenhouse gases g_{t-1} and the *land sink absorption rate*, $\rho_t \equiv s_t^{lan}/\omega_{t-1}^{lan}$, the land sink per unit of land stock, entering period t. The absorption rate ρ_t can be either positive or negative, taking values in $[-1, \infty)$. Negative values correspond to respiration and decomposition rates that exceed in total the rate of photosynthesis. At low atmospheric concentrations, increases in CO2e in the atmosphere increases the activation energy in plant photosynthesis. Consequently, carbon uptake (photosynthesis net of plant respiration) rises. After some point, however, increased GHG concentrations become toxic and/or higher temperatures deplete nutrient and moisture retention which further reduces uptake. Related mechanisms are studied by Fernandez-Martinez et al. (2017), Thomson et al. (2008), and Feng et al. (2015). To account for these effects, we posit

$$\rho_t \equiv \frac{s_t^{lan}}{\omega_{t-1}^{lan}} = F(g_{t-1}; \pi) \tag{2}$$

where F is a continuous function of g_{t-1} and π is a vector of parameters. We refer to F as the *sink absorption function*. We later postulate and estimate the parameter vector π for a flexible absorption function. To isolate the effects on land carbon, the

[4]Following upgraded measurement, the United Nation's new designation is "Land use, land use change, and forestry" (LULUCF), though the original terminology still dominates the literature.

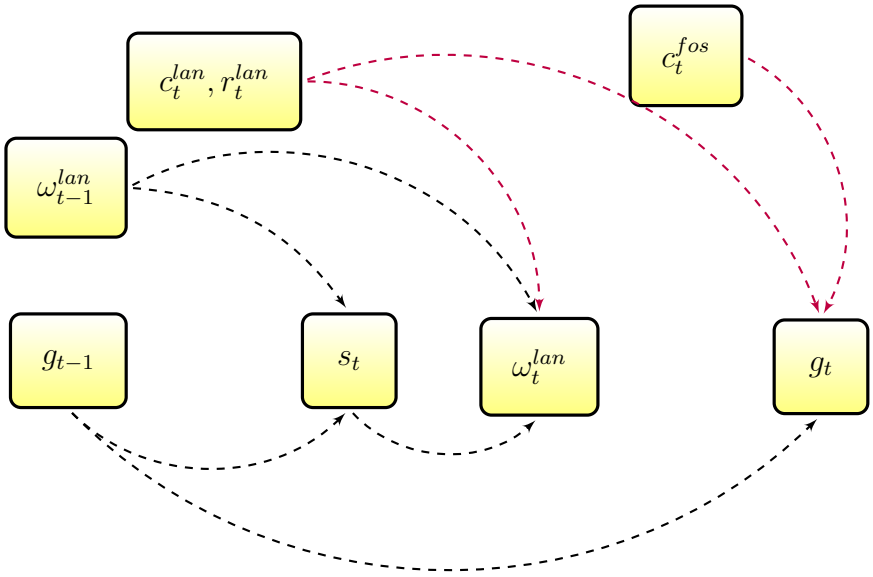

Figure 1: Rudimentary Land-Atmosphere Carbon Cycle.

sink absorption function (2) is the only feedback mechanism in the model. Other feedback effects on, say, marine ecosystems, are not incorporated.

Let c_t^{fos} denote fossil fuel consumption at t. Combining Equations (1) and (2) with a mass balance of carbon reservoirs, one obtains a rudimentary version of the land-atmospheric carbon cycle. The channels for this cycle are illustrated in Figure 1.

2.2 Output and Equilibrium Land Use Policies

Land emissions and removals are choices made by countries and depend on the country's stock of terrestrial carbon found in biomass and soils. Adding an "i" subscript to each of the variables, we obtain country i's land carbon stock ω_{it}^{lan} at the end of period t. We also obtain i's land emissions c_{it}^{lan}, fossil fuel emissions c_{it}^{fos}, its atmospheric removals r_{it}^{lan}, and its land sink s_{it}^{lan}. These aggregate to global levels as expected: $\omega_t^{lan} = \sum_i \omega_{it}^{lan}$, $c_t^{fos} = \sum_i c_{it}^{fos}$, $c_t^{lan} = \sum_i c_{it}^{lan}$, $r_t^{lan} = \sum_i r_{it}^{lan}$, and $s_t^{lan} = \sum_i s_{it}^{lan}$.

The country-specific version of the land stock dynamic in Equation (1) is

$$\omega_{it}^{lan} = \omega_{i\,t-1}^{lan} - (c_{it}^{lan} - r_{it}^{lan}) + s_{it}^{lan}. \tag{3}$$

Like their global counterparts, c_{it}^{lan} incorporates activities such as harvesting, soil drainage, and deforestation within country i, while r_{it}^{lan} includes replanting, reseeding, and reforestation. The land sink s_{it}^{lan} of country i represents non-anthropogenic removals from the atmosphere that feed directly into the country's land stock.

At the country level, human activities enter into a country's output each period. The output y_{it} of country i is generated by the production function

$$y_{it} = A_i \varepsilon_{it} (c_{it}^{lan})^{\alpha_i} (\omega_{it}^{lan})^{\beta_i} (c_{it}^{fos})^{\gamma_i} H_{it}^{\zeta_i} L_{it}^{\eta_i}. \tag{4}$$

In this expression A_i is a TFP scale parameter for country i, and ε_{it} is a log normally distributed iid shock with mean 1. The inputs are land use c_{it}^{lan}, land stock ω_{it}^{lan}, fossil fuel consumption c_{it}^{fos}, labor L_{it}, and a capital-emissions intensity variable H_{it}. The input H_{it} is a TFP component, defined as the ratio, $\frac{K_{it}}{c_{it}^{fos}}$, where K_{it} is the capital stock of country i. Input H_{it} captures various technological changes over time. These changes are distinguished in a Kaya-like decomposition of H_{it},

$$H_{it} \;=\; \frac{K_{it}}{c_{it}^{fos}} \;=\; \frac{K_{it}}{E_{it}} \times \frac{E_{it}}{c_{it}^{fos}}, \tag{5}$$

where E_{it} is the energy usage (in GJ) of country i in t. Assumptions about future changes in ratios $\frac{K_{it}}{E_{it}}$ and $\frac{E_{it}}{c_{it}^{fos}}$ are common in climate models and IAMs. We return to these later on.

Notice that while physical capital K_{it} does not directly enter the production equation (4), variations in capital are jointly captured by variations in fossil fuel emissions c_{it}^{fos} and the capital-emissions intensity H_{it}. We point out in fact that when $\beta_i = 0$ and $\gamma_i = \zeta_i$, the output model (4) reduces to

$$y_{it} = A_i \varepsilon_{it} (c_{it}^{lan})^{\alpha_i} K_{it}^{\zeta_i} L_{it}^{\eta_i}.$$

In other words, a special case of (4) is the standard Cobb-Douglas production model with the usual inputs: capital, labor, and land. The special case where $\beta_i = 0$ conforms to a more traditional resource model in which carbon stock matters only

through its consumption.[5] The model allows for $\beta_i = 0$ and even $\beta_i < 0$.[6] One might nevertheless expect direct and positive effects of land stock ($\beta_i > 0$) due to improved soil nutrition, drainage, erosion prevention, flood control, waste filtration, and climate stabilization. In addition, the possibility that $\gamma_i \neq \zeta_i$ allows for output to respond differently to fossil fuel consumption and to emissions-reducing improvements in the use of capital.

The effects of GHG emissions enter Equation (4) through its effect on land carbon stock. The details of the radiative forcing process are omitted. By contrast, IAMs, damage to GDP from climate change is postulated as an increasing function of global surface temperature. In turn, surface temperature increases with greenhouse gas (GHG) concentrations from energy use. A canonical representation is the DICE model (e.g., Nordhaus (2018)). There, the damage function negatively enters the TFP component in a standard production technology. Parameter values of the damage function are fixed or estimated from external studies and then used to calibrate the long run effects of climate change on output.

Combining the output Equation (4) with the law of motion for carbon stock in Equation (3), we obtain

$$y_{it} = A_i \varepsilon_{it} (c_{it}^{lan})^{\alpha_i} \left(\omega_{i\,t-1}^{lan} - c_{it}^{lan} + r_{it}^{lan} + s_{it}^{lan}\right)^{\beta_i} (c_{it}^{fos})^{\gamma_i} H_{it}^{\zeta_i} L_{it}^{\eta_i}. \tag{6}$$

Land consumption c_{it}^{lan} appears as both a direct and indirect input, the latter entering negatively through the land stock.

A policymaker from country i maximizes the discounted long run payoff

$$\sum_{t=0}^{\infty} \delta^t \left[\log(y_{it}) + \theta_i \log(\omega_{i\,t-1}^{lan} - r_{it}^{lan})\right]. \tag{7}$$

given (6). Equation (7) is a reduced form payoff defined directly over output. The first term is i's flow payoff from y_{it}. The second term is its payoff from services derived from land stock net of investments (removals) to expand it. This term is the payoff from home production or, alternatively, the payoff from eco-services

[5] In pure extraction models, e.g. Levhari and Mirman (1980), Cave (1987), Fisher and Mirman (1992), conservation is valued for instrumental reasons: preserving the stock allows the decision maker to smooth consumption. The non-instrumental trade offs modeled are somewhat similar to models of Dutta and Radner (2004, 2006, 2009) who study dynamic strategic models of energy usage with emissions externalities, and Harrison and Lagunoff (2017, 2019) who also incorporate carbon stock as productive input.

[6] At a local level, invasive plant species could produce $\beta_i < 0$. The equilibrium conditions introduced later on will imply restrictions on the sum $\alpha_i + \beta_i$.

including tourism, outdoor leisure, and general enjoyment of green space. Home production is relevant in developing countries where the land ecosystem is a non-monetized input that maintains soil stability, water filtration, and so on. This second term is assumed decreasing in r_{it}^{lan}, reflecting the cost of augmenting and reseeding the stock. Without this cost, the policymaker would arbitrarily scale up removals, thereby allowing infinite consumption of land carbon.

At each date, the policy maker chooses land activities c_{it}^{lan} and r_{it}^{lan}. The assumption that land activities are policy choices contrasts with most models of land use where activities are determined in a perfectly competitive market.[7] The reality is that most national governments exercise substantial power over their countries' land stocks. In many countries the bulk of carbon biomass is on nationally owned land. In China, for instance, more than half of its territory and nearly all its forest land is publicly owned by the state. In the U.S. 28% of its territory is nationally held, and this excludes property held by various state governments (Rights and Resources Initiative, 2015; Vincent, Hanson, and Argueta, 2017). Even when property is privately held, federal laws governing private and public takings, pollutants, forestry, water and waste management, zoning restrictions, safety, building codes, and an array of subsidies and taxes implicate government in virtually all forms of land use.

The collection of land use decisions constitutes a dynamic game among countries. A *land carbon policy* for country i is a pair of Markov strategies $\mathbf{c_i^{lan}}$ and $\mathbf{r_i^{lan}}$ that map at each date from the initial stock $\omega_{i\,t-1}^{lan}$ and land sink s_{it}^{lan} to land use c_{it}^{lan} and removals r_{it}^{lan}, respectively. A *Markov Perfect equilibrium (MPE)* describes a land policy for each country that maximizes its representative citizen's long run payoff (7) at each t for every stock, given land policies of other countries.[8]

By construction, the collection of land policies constitutes an MPE if, given the land policies of other countries, each country's land policy satisfies the Bellman

[7]Detailed dynamic modeling of land use is found in the dynamic Global Trade Analysis Project (GTAP), include Golub, Hertel, and Sohngen (2008).

[8]MPE are Subgame Perfect equilibria in Markov strategies. The formal definition and notation are omitted for brevity.

equation

$$
\begin{aligned}
V_i(\mathbf{c_i^{lan}}, \mathbf{r_i^{lan}}; \omega_{i\,t-1}^{lan}, s_{it}^{lan}) \;=\; \max_{c_{it}^{lan}, r_{it}^{lan}} \Big\{ & \alpha_i \log(c_{it}^{lan}) \;+\; \beta_i \log\left(\omega_{i\,t-1}^{lan} + r_{i,t}^{lan} + s_{it}^{lan} - c_{it}^{lan}\right) \\
& +\; \theta_i \log(\omega_{i\,t-1}^{lan} - r_{it}^{lan}) \;+\; \gamma_i \log(c_{it}^{fos}) \;+\; \zeta_i \log(H_{it}) \;+\; \eta_i \log(L_{it}) \\
& +\; \delta\; E\left[V_i(\mathbf{c_i^{lan}}, \mathbf{r_i^{lan}}; \omega_{i\,t}^{lan}, s_{i\,t+1}^{lan})\right] \;\Big\} \\
& \text{subject to sink absorption function (2).}
\end{aligned}
\tag{8}
$$

Equation (8) excludes the constant term $\log(A_i)$ and current log productivity shock $\log(\epsilon_{it})$. Under the log normal assumption the shock does not figure in the policymaker's decision problem.

In the MPE, countries consider the both structural and strategic consequences of their land use emissions and removals, the latter via net increases in atmospheric stock g_t. To simplify the equilibrium, each country solves its Bellman equation assuming its effect on the aggregate state is negligible. Specifically, each country chooses its land policy assuming that $\frac{\partial g_t}{\partial c_{it}^{lan}} = \frac{\partial g_t}{\partial r_{it}^{lan}} = 0$. The "Negligibility" assumption is a reasonable approximation of the empirical relationship. At any given time, a country's LUCF is a small fraction of global emissions and a minuscule fraction of total atmospheric GHGs.[9] Negligibility simplifies the model by breaking down the game into a collection of interacting dynamic optimization problems.

We refer to the collection $(\mathbf{c_i^{lan}}, \mathbf{r_i^{lan}}),\;\; i = 1, \ldots, n$ that solve the Bellman equation for each i under Negligibility as simply an *equilibrium*.[10]

The following proposition establishes that the country's Bellman equation admits a simple closed form solution:

[9] In 2015, for instance, total fossil fuel emissions by the U.S. constituted the fraction 8.332E-9 of total GHG concentrations.

[10] An equilibrium by this definition can be shown to be an approximate Markov Perfect equilibrium in the sense that the equilibrium converges uniformly to a full MPE as the true marginal effects of one's land policy on total atmospheric concentrations converge to zero. The assumption does not imply that a country regards its own land sink as exogenous. By Equation (2), land sinks are proportional to carbon stock, and the effects of an incremental change in its own carbon stock are fully internalized by the country.

Proposition 1 *In any equilibrium, each country's land carbon policy is given by*

$$\begin{aligned} \mathbf{c}_{it}^{lan}(\omega_{i\,t-1}^{lan}, s_{it}^{lan}) &= \frac{\alpha_i(1-\delta)(2\omega_{i\,t-1}^{lan} + s_{it}^{lan})}{\alpha_i + \beta_i + \theta_i} \\ \mathbf{r}_{it}^{lan}(\omega_{i\,t-1}^{lan}, s_{it}^{lan}) &= \omega_{i\,t-1}^{lan} - \frac{\theta_i(1-\delta)(2\omega_{i\,t-1}^{lan} + s_{it}^{lan})}{\alpha_i + \beta_i + \theta_i}. \end{aligned} \tag{9}$$

The equilibrium exists whenever $\alpha_i > 0$ *and* $\alpha_i + \beta_i + \theta_i > 0$ *for each* i*. If* $\beta_i > 0$*, then* $\theta_i > 0$*.*

The derivation of (9) is in Appendix 7.1. A country's equilibrium land emissions and removals are multilinear functions of lagged land stock $\omega_{i,t-1}^{lan}$ and current land sink s_{it}. Emissions (removals) are decreasing (increasing) in the discount factor since the upside to removals comes in the future.

Recall that α_i, the production coefficient on land emissions, represents that output responsiveness to increases in land use. Both emissions and removals are increasing in α_i. The increase in removals owes to the fact that removals represent a re-investment in land carbon that enables increased land consumption in the future.

Parameter β_i, the coefficient on land stock, represents output responsiveness to the ecosystem. Emissions (removals) are decreasing (increasing) in β_i.

Existence of equilibrium requires some parametric restrictions. If $\alpha_i \leq 0$ then the country should generate no land use emissions. If $\beta_i > 0$ and $\theta_i \leq 0$ then the country should accumulate an unbounded volume of biomass. If $\alpha_i + \beta_i + \theta_i < 0$, then the country should immediate deplete its land stock. Payoffs are ill-defined in all these cases.

Note that the cases $\beta_i < 0$, and even $\alpha_i + \beta_i < 0$ are consistent with existence of an equilibrium land policy. Changes in land stock can be negatively related to *measured* GDP growth due the presence of home/non-monetized production. With home production, a reduction in land biomass can lead to greater substitution toward monetized output and away from home production. This "substitution effect" is likely more prevalent in developing countries and could produce a sum $\alpha_i + \beta_i$ that's negative. In that case, θ_i must be large relative to $|\beta_i|$ so that the sum $\alpha_i + \beta_i + \theta_i$ remains positive.

Later on, the model is specialized to the case where land sink absorption rates $s_{it}^{lan}/\omega_{t-1}^{lan}$ are identical across countries. In that case equilibrium land policies in (9)

can be alternatively expressed simply as

$$\begin{aligned} \mathbf{c}_{it}^{lan}(\omega_{i,t-1}^{lan}, \rho_t) &= \frac{\alpha_i(1-\delta)\omega_{i,t-1}^{lan}(2+\rho_t)}{\alpha_i+\beta_i+\theta_i} \\ \mathbf{r}_{it}^{lan}(\omega_{i,t-1}^{lan}, \rho_t) &= \omega_{i,t-1}^{lan} - \frac{\theta_i(1-\delta)\omega_{i,t-1}^{lan}(2+\rho_t)}{\alpha_i+\beta_i+\theta_i}. \end{aligned} \tag{10}$$

Equation (10) displays the sensitivity of land use policies to changes in the land sink absorption rates.

3 Structure and Identification

The assumption of our empirical strategy is that the countries in the sample behave as the equilibrium described above. The structural parameters in the production model are $\alpha_i, \beta_i, \gamma_i, \zeta, \eta_i, \theta_i$, and the TFP parameter, A_i. In principle, these would be identified from the transition rule (3), the output equation (either (4) or (6)), and the pair of equilibrium land policy equations in (10) over a long enough time series.

One concern is that the equilibrium policy rules are all linear in stocks. A related problem comes from the data itself. Available data on land policies does not, to our knowledge, separate out land consumption c_{it}^{lan}, land removals r_{it}^{lan}, and land sink s_{it}. All three are combined in measurements of *net* emissions from land after accounting for removals and sinks. However, only consumption (as measured by emissions) generates current production. To address these problems, equilibrium land use policies in (9) are incorporated directly into the output equation (6) to produce a tractable "reduced form" equation in variables for which there is data. This yields the following equation system expressed in natural logs:

$$Y_{it} \;=\; constant_i \;+\; B_i X_{i1t} \;+\; \gamma_i X_{2it} \;+\; \zeta_i X_{3it} \;+\; \eta_i X_{4it} \;+\; \epsilon_{it} \tag{11}$$

where

$$Y_{it} = \log(y_{it}) \tag{12}$$

$$X_{it1} = \log\left(2\omega_{i\,t-1}^{lan} + s_{it}^{lan}\right) \tag{13}$$

$$s_{it}^{lan} = \omega_{i\,t-1}^{lan}\rho_t \tag{14}$$

$$X_{2it} = \log(c_{it}^{fos}) \tag{15}$$

$$X_{3it} = \log(H_{it}) \tag{16}$$

$$X_{4it} = \log(L_{it}) \tag{17}$$

$$constant_i = \log(A_i) + \alpha_i \log\left(\frac{\alpha_i(1-\delta)}{\alpha_i+\beta_i+\theta_i}\right) + \beta_i \log\left(1 - \frac{(1-\delta)(\alpha_i+\theta_i)}{\alpha_i+\beta_i+\theta_i}\right) \tag{18}$$

$$B_i = \alpha_i + \beta_i \tag{19}$$

and

$$\epsilon_{it} = \log(\varepsilon_{i,t}) \tag{20}$$

In the equation system (11)-(20) the main explanatory variable X_{1it} is a log composite of one-period lagged carbon stock $\omega_{i\,t-1}^{lan}$ and land sink s_{it}^{lan}. In turn, the country's land sink s_{it}^{lan} is a product of its lagged stock $\omega_{i,t-1}^{lan}$, and absorption rate ρ_t. Variables X_{2it},X_{3it}, and X_{4it} are logs of c_{it}^{fos}, H_{it}, and L_{it} and respectively.

Equation (14) follows from a simplifying assumption that the sink absorption function F in Eq. (2) is the same for all countries. The country absorption rates are then computed from global absorption rates according to $\rho_t = s_{it}^{lan}/\omega_{i,t-1}^{lan}$ for each country i. Since ρ_t is observed directly, the functional form of F and the parameter vector π is not needed for the output estimation. But these will be needed later on for the simulation exercise.

The key parameters α_i and β_i are not point identified. However, the sum $B_i = \alpha_i + \beta_i$ is. As pointed out earlier this follows from the fact that equilibrium policies c_{it}^{lan} and r_{it}^{lan} are collinear in the lagged stock $\omega_{i\,t-1}^{lan}$. The other production coefficients are identified. For purposes of pinning down equilibrium policies, the sum B_i would suffice were it not for payoff parameter θ_i which is also not identified. It appears in the constant term, as do pre-determined parameter δ and A_i. However, since the

data limitation prevents one from observing the individual policies in any event, we are left to focus on the equilibrium "reduced form" equation (11) for GDP. This equation can be pinned down up to a scale constant that can be estimated alongside coefficient B_i and the remaining structural parameters.

Clearly, $B_i = \alpha_i + \beta_i$ is the coefficient of interest. It approximates a *policy-adjusted output elasticity* under equilibrium land use. The policy-adjusted elasticity is derived from the following terms. Let $y_i^*(\omega_{i,t-1}^{lan}, s_{it}^{lan})$ denote the indirect production function when equilibrium land use policies $\mathbf{c}_{it}^{lan}(\omega_{i,t-1}^{lan}, s_{it}^{lan})$ and $\mathbf{r}_{it}^{lan}(\omega_{i,t-1}^{lan}, s_{it}^{lan})$ are in place. Carbon stock enters both as a direct input and as an indirect input via the equilibrium land use. The combination of the two in the log output equation yields

$$\begin{aligned}\alpha_i \log(\mathbf{c}_{it}^{lan}(\omega_{i,t-1}^{lan}, s_{it}^{lan})) + \beta_i \log\left(w_{i,t-1}^{lan} - \mathbf{c}_{it}^{lan}(\omega_{i,t-1}^{lan}, s_{it}^{lan}) + \mathbf{r}_{it}^{lan}(\omega_{i,t-1}^{lan}, s_{it}^{lan})\right) + s_{it}^{lan}\right) \\ = (\alpha_i + \beta_i)\log(2\omega_{i,t-1}^{lan} + s_{it}^{lan}) = (\alpha_i + \beta_i)\log(\omega_{i,t-1}^{lan}(2+\rho_t)) \equiv B_i X_{i1t} \quad (21)\end{aligned}$$

The last line in (21) follows from Equations (2) and (14). In this expression, the composition of shares in y_i^* into ecosystem and land consumption are described by the combined term $B_i X_{i1t}$. From the term $B_i X_{i1t}$, one derives the *policy-adjusted (output) elasticity* of the y_i^* with respect to lagged carbon stock ω_{t-1}^{lan}. The policy-adjusted elasticity, comprising a combination of direct and indirect changes in carbon stock, is approximated by B_{i1}. Specifically,

$$\left(\frac{\partial y_i^*}{\partial \omega_{i,t-1}^{lan}}\right)\left(\frac{\omega_{i,t-1}^{lan}}{y_i^*(\omega_{i,t-1}^{lan}, s_{it}^{lan})}\right) \approx B_i \equiv \alpha_i + \beta_i \quad (22)$$

Overall, land stocks are altered by carbon sink absorption and absorption rates are, in turn, altered due to GHG concentrations. B_{i1} then approximates the response in current output to increased GHGs.

4 Quantifying the Effects of Land Carbon

4.1 Overview

This section quantifies the effects of land carbon on GDP in the system of equations (11)-(20). Subsection 4.2 describes the data. Subection 4.3 contains estimates of the production parameters. The estimated parameters, along with those of a land sink absorption function, are subsequently used as calibrating parameters in the simulations in Section 5. A complete description of sources and constructions are in Appendix 7.4.

4.2 The Data

The relevant times series are the country and global land stocks, $\{\omega_{it}^{lan}\}$ and $\{\omega_{t}^{lan}\}$, resp., the country and global land sinks $\{s_{it}^{lan}\}$ and $\{s_{t}^{lan}\}$, resp., global GHG atmospheric stock $\{g_t\}$, country-specific output $\{y_{it}\}$, fossil fuel consumption $\{c_{it}^{fos}\}$, capital-emissions ratio $\{H_{it}\}$, and labor force $\{L_{it}\}$. Data for these time series spans 152 countries covering the time period 1990-2015.

Our data is constructed from sourced data by modifying stock and flow data to conform with U.N. reporting requirements. Specifically, FAOSTAT, the U.N. Food and Agricultural Organization's database and the source for the country land carbon stock series, $\{\omega_{it}^{lan}\}$, publishes updates of country data *every five years*. These updates are based on U.N. reporting requirements for countries. Hence, from here on the dates t will range over the 5 year increments. i.e, $t = 1990, 1995, 2000, 2005, 2010, 2015$. This presents no problem for the theory since the model is agnostic about the length of a decision period. The notation "τ" will be used to represent annual time periods. Data on stocks $\{\omega_t, \omega_{it}^{lan}, g_t, H_{it}, L_{it}\}$ are then reported at quinquennial dates t. The data on flows are also reported at quinquennial dates t but represent aggregates over the past five years, up to and including the quinquennial date. Consequently, the flow data represented by a "tilde" on the variables are defined as

$$\tilde{s}_t^{lan} = \sum_{\tau=0}^{4} s_{t-\tau}^{lan}, \quad \tilde{c}_{it}^{fos} = \sum_{\tau=0}^{4} c_{t-\tau}^{fos}, \quad \tilde{y}_{it} = \sum_{\tau=0}^{4} y_{t-\tau} \tag{23}$$

for $t = 1990, 1995, 2000, \ldots, 2015$. In addition,

$$\tilde{\rho}_t \equiv \frac{\tilde{s}_t^{lan}}{\omega_{t-5}^{lan}} \quad \text{and} \quad \tilde{s}_{it}^{lan} = \tilde{\rho}_t \, \omega_{i,t-5}^{lan} \tag{24}$$

are the quinquennial analogues of the earlier specification. The absorption rate is applied to individual countries.

A summary of the variables, measurement units, and sources are listed in Table 1. These variables will those used to estimate the equation system (11)-(20). Regarding units of measurement listed in the Table, atmospheric stocks include carbon and non-carbon GHGs, measured in gigatonnes (Gt) of carbon dioxide equivalent (CO2e). Units of CO2e convert all green house gases into CO2 by measuring Global Warming Potential, a relative measure of how much heat a greenhouse gas traps in the atmosphere.[11] Raw data on land stocks and flows include only carbon, but are

[11] Definitions and conversion factors are provided in the Appendix.

converted to Gt CO2e units only for the purpose of having a simple, common unit of account. Land stocks and flows are kept separate from GHG measurements that include non-carbon sources. Full details on units of measurement, conversion factors, data sources, and constructions are in Appendix 7.4.

Table 1: Summary of Data Variables.

Symbol	Units	Description	Source
ω_t^{lan}	Gt CO2e	Global carbon stock	Global Carbon Project
ω_{it}^{lan}	Gt CO2e	Country i carbon stock	FAOSTAT
g_t	Gt CO2e	Global GHG (incl. non-carbon sources)	NOAA
$\tilde{s}_t^{lan}$	Gt CO2e	Global land carbon sink - last 5 yrs	Global Carbon Project
$\tilde{s}_{it}^{lan}$	Gt CO2e	Country i land carbon sink - last 5 yrs	calculated in Eq. (24)
$\tilde{c}_{it}^{fos}$	Gt CO2e	Country i fos. fuel emit. over last 5 yrs	World Resources Inst.
K_{it}	10^{12} PPP 2011 USD	country i capital stock	Penn World Tables 9.1
H_{it}	$K_{it}/\tilde{c}_{it}^{fos}$	capital stock-emissions ratio	calculation
L_{it}	population	Country i labor force	World Bank
$\tilde{y}_{it}$	10^{12} PPP 2011 USD	Country i GDP over last 5 yrs	World Bank

All stocks are end-of-quinquennial time period. Variables with "tildes" are aggregates of annual flows over the five year year period up to and including the quinquennial year.

4.3 Production Parameters

We group countries according to the United Nation's Human Development Index (HDI). The HDI formulates criteria for four distinct country groups: High Development, Medium High Development, Medium Low Development, or Low Development (United Nations Development Programme, 2019). The HDI partition allows for heterogeneous production according to different levels of development while also maintaining large enough sample sizes within each cluster to obtain meaningful estimates. We cross-check our results against other clustering strategies and other model specifications.

The production coefficients are assumed identical across all countries within each development group k where $k = H, MH, ML, L$. We also consider the global cluster $k = world$. The estimating equation (11) then reduces to

$$Y_{it} \;=\; constant_i \;+\; B_k X_{i1t} \;+\; \gamma_k X_{2it} \;+\; \zeta_k X_{3it} \;+\; \eta_k X_{4it} \;+\; \epsilon_{kt} \tag{25}$$

for country i in HDI cluster k with $B_k = \alpha_k + \beta_k$, and all variables are defined by the equation system (11)-(20).

Table 2: Policy-Adjusted Elasticities by HDI Cluster.

	Dependent Variable - Log GDP				
Coefficients	High	Medium High	Medium Low	Low	All
B Carbon Stock	0.250***	0.946***	0.050	0.109	0.294***
	(0.081)	(0.174)	(0.152)	(0.098)	(0.062)
γ Fossil Fuel	0.769***	1.083***	1.103***	0.861***	0.992***
	(0.092)	(0.113)	(0.106)	(0.099)	(0.054)
ζ K/c^{fos} ratio	0.355***	0.132***	0.184***	0.174***	0.242***
	(0.023)	(0.038)	(0.040)	(0.124)	(0.016)
η Labor Force	-0.050	0.096	0.289**	0.496***	0.136**
	(0.081)	(0.162)	(0.168)	(0.132)	(0.069)
Observations	184	168	136	120	608
R^2	0.998	0.995	0.996	0.993	0.997
F Statistic	1459.2	513.2	619.3	627.1	834.4

Includes Country-Fixed Effects. Standard errors in parentheses. Symbols *, **, and *** indicate statistically significant at the 10%, 5%, and 1% levels, respectively. Based on Human Development Index (HDI), U.N. Development Programme. #Observations = # countries in cluster × 4 lagged quinquennial time periods up to 2015.

We control for country-specific fixed effects by maintaining heterogeneity of the constant term (via the scale term A_i). The main focus is the policy-adjusted output elasticity of land carbon stock B_k. Results are in Table 2. The last column refers to the global cluster (all countries in a single grouping). The estimates for B_k are all positive and are statistically significant in the High or Medium High development clusters and in the global cluster.[12] Estimates of B_k for lower development countries are positive but not significantly different from zero. Estimates of elasticities of fossil fuel emissions and capital-to-emissions ratios for all clusters are all significant.

The policy-adjusted elasticity approximates the incremental effects of land carbon stock on annual GDP. Using the global cluster, a 1% increase (decrease) in global land carbon is associated with a roughly 0.29% increase (decrease) in annual GDP over the five year period following the change in carbon stock. The change in GDP includes the effects of both the increased (decreased) land consumption and the altered ecosystem.

At a more disaggregated level, consider a country in the High development cluster. A 1% increase in its land carbon is associated with a 0.25% increase in total GDP over the next five year period. In the U.S. the observed increase land carbon stocks

[12]Unless otherwise stated, the references to statistically significance in the text refer to the 1% level.

from 2011 to 2015 was, in fact, around 1.5%. Based on a conservative estimate for its five year U.S. GDP in the quinquennial period 2016-2020 of 94 trillion (2017 constant dollars), the increase would account for around 0.353 trillion USD.

In China, a country in the Medium High cluster, the effects are substantially larger. A 1% increase in its land carbon is associated with a 0.946% increase in total GDP the next five year period. The observed increase in Chinese land carbon from 2011-2015 was 6.7%. Applied to an estimated five year GDP of 61 trillion from 2015-2020, the increase in land carbon stock accounted for roughly 3.87 trillion USD.

Of the change in land carbon stocks, around two thirds was due to reductions in land emissions and/or increases in removals. The other third is from the land sink. Consequently, any large reductions in land sink absorption rates over the next few decades could have sizable cumulative effects on GDP in High and Medium High countries.

Robustness. We compare the estimates in Table 2 to those for several other partitioning/clustering strategies. These are described in an online appendix and support findings in Table 2 that estimated policy-adjusted land carbon elasticity B is statistically significant for groupings dominated by developed countries. Groups where the estimated B is indistinguishable from zero consist of highly forested countries in subsaharan Africa and Asia. The higher initial resource stock and lower level of development may have rendered these country's outputs less responsive to changes in the ecosystem thus far.[13]

In addition, we examine some alternative model specifications. We note that both carbon stocks and GDP have generally increased in developed countries since 1990. Whereas, in low development countries, GDP has generally increased while carbon stocks in some heavily forested countries declined or remained flat. In principle, this time trend could account for significant land carbon estimates in High but not Low HDI countries. This raises the question of whether the land carbon-output association is explained by an omitted variable reflected in time trend in the sample period.

It turns out this is unlikely. Much of the trend can be accounted for in the capital emissions ratio H_{it} which trends upward in most countries, but especially in developed countries. To confirm this, we evaluate two alternative specifications. In the first alternative, we shut down the trend in H_{it}, assuming it to be constant over

[13]The model does not address other ways in which developing countries may be vulnerable to climate change. See Althor, Watson, and Fuller (2016) and other references in the Introduction.

time. In the second alternative, we substitute a pure time trend variable in place of H_{it}. The estimates for both these alternative specifications are reported in Tables 6 and 7 in Appendix. 7.5. In both alternative specifications, the land carbon elasticity estimate remains significant for the High and Medium High Development countries. This indicates that the correlation between land carbon and GDP is not simply due to time trend and that H_{it} reasonably controls for it.

5 Simulated Time Paths for 2020-2100

This section describes details and results of an exercise to simulate the model time paths for land carbon stocks and GDP over all country clusters. Subsection 5.1 estimates a parametric absorption function in an "active" sink model (with potentially declining sink rates), and a constant sink model. The simulation incorporates the estimated parameters under both models for each of the four standard *Representative Concentration Pathways (RCPs)* developed by research teams for IPCC's Fifth Assessment Report, 2014. Subsection 5.2 describes the simulation algorithm. Subsection 5.3 describes the RCP scenarios in the IPCC's report. Using the algorithm, future land sink absorption rates are forecasted in each scenario and under different land sink specifications. Subsection 5.4 displays simulation results for land stocks. Subsection 5.5 displays simulation results for GDP.

5.1 Land Sink Absorption Parameters

We first estimate a parametric form of land sink absorption function F in (2). Assume F satisfies

$$\log(\tilde{\rho}_t + 1) \;=\; \pi_0 \;+\; \pi_1\, g_{t-5} \;+\; \pi_2\, g_{t-5}^2 \;+\; \mu_t \tag{26}$$

Equation (26) posits $\tilde{\rho}_t$, the absorption rate defined in (24), as a Gaussian function of lagged GHG concentrations. The Gaussian function satisfies boundary conditions, and if $\pi_2 < 0$ then the crucial property that sink absorption is an inverted-U function of concentrations is satisfied. The unit adjustment to $\tilde{\rho}_t$ in the log term adjusts for the fact that $\tilde{\rho}_t$ can be negative, as long as $\tilde{\rho}_t > -1$. Unlike a quadratic which falls rapidly after reaching a peak, the value of $\tilde{\rho}_t$ in (26) gradually declines and converges slowly to its lower bound. μ_t is a mean zero disturbance in the sink rate, assumed uncorrelated with concentrations.

Table 3: Estimated Parameters of Sink Absorption Equation (26).

	π_0	π_1	π_2
Land sink parameter	-0.500**	3.02E-4**	-4.19E-8**
	(0.277)	(1.65E-4)	(2.44E-8)
R^2	0.485		
F-stat	12.7		
Model P-value	1.3E-4		

Standard errors in parentheses. Symbols *, **, and *** indicate statistically significant at the 10%, 5%, and 1% levels, respectively. The sample period covers 1987-2016 for sink absorption rates, and 1982-2011 for quinquennially lagged GHG concentrations. The full description is in Appendix 7.6.

We refer to Equation (26) as the *active sink model* in order to contrast it with the a *constant sink model* in which the absorption rate is held fixed at its empirical average value $\rho = 0.043$ over the sample period. The estimated values $\hat{\pi}_0, \hat{\pi}_1, \hat{\pi}_2$ of the active sink model, reported in Table 3, are significant (5% level). Moreover, the negative coefficient π_2 provides support for inverted-U sink absorption function in which terrestrial carbon uptake (photosynthesis net of plant respiration) rises then falls (Hikosaka et al. (2006), Thomson et al. (2008), Raupach et al. (2014), Xu (2015), Feng et al. (2015) Fernandez-Martinez et al. (2017), and Zheng et al. (2018)). In the fitted absorption function, the global absorption rate reaches a maximum at atmospheric stock around $g_t = 3650$ Gt CO2e (467.35 ppm CO2e) and declines thereafter. This is lower than peak CO2 absorption at constant temperatures (Xu (2015) and Thomson et al. (2008)), suggesting that climate plays a role. Specifically, separating out climate change effects from the pure toxicity/nutrient effects, the former also contributes to reduced sink capacity. The fitted active and constant sink equations are displayed against GHG concentrations data in Figure 2.

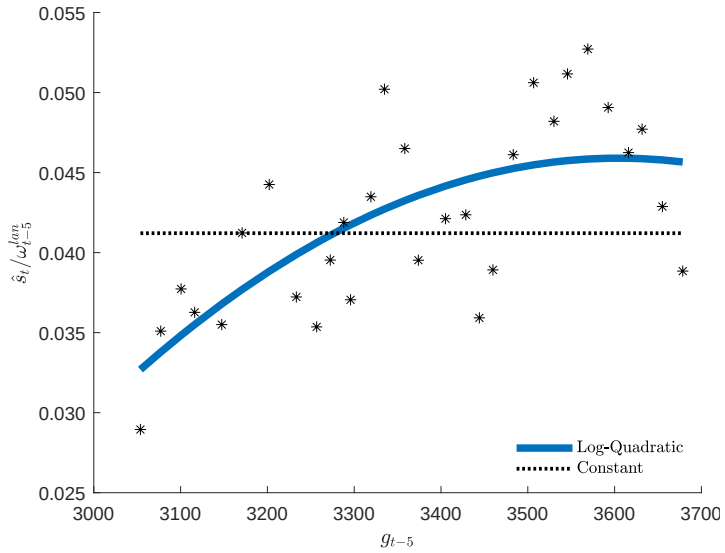

Figure 2: Estimated Land Sink Absorption Function.

We later run simulations in both active and constant sink models, the latter to obtain a benchmark for measuring the feedback effects in the model.

5.2 The Simulation Algorithm

Using the estimates as calibrated parameters, we simulate the model for each of the four Representative Concentration Pathways (RCPs). The meaning and interpretation of the RCPS are described in the next subsection. From the source data for each RCP, we construct a forecast $\{g_{t,\,RCP}\}$ for atmospheric stocks, for country emissions $\{\tilde{c}^{fos}_{it,RCP}\}$, and for capital-emissions ratios $\{H_{it,RCP}\}$. Using these, along with a forecasted labor series $\{L_{it}\}$, we simulate dynamic paths, $\{\tilde{y}_{it,RCP}\}$, $\{\omega^{lan}_{it,RCP}\}$, and $\{\tilde{s}^{lan}_{it,RCP}\}$, $t = 2020, 2025, 2030, \ldots, 2100$.

The simulation algorithm produces model-generated series for land stocks and GDP as follows: Step (i): construct the predicted global land sink absorption series $\left\{\frac{\widetilde{s^{lan}_{t,RCP}}}{\omega^{lan}_{t-1,RCP}}\right\}$ from the land sink estimation given parameter estimates $\hat{\pi}_0$, $\hat{\pi}_1$, and $\hat{\pi}_2$; Step (ii): recursively generate the series for land stocks $\{\omega^{lan}_{it}\}$ from the model law of motion under estimated parameters in equilibrium; Step (iii): generate model paths of GDP from the estimated parameters $\hat{B}_k, \hat{\gamma}_k, \hat{\zeta}_k$ and $\hat{\eta}_k$ for cluster k and given the series $\{\tilde{c}^{fos}_{it,RCP}\}$, $\{H_{it,RCP}\}$, and $\{L_{it}\}$. Details of the RCP source data, our

constructions derived from it, and the simulation algorithm is in Appendix 7.7.

5.3 RCPs and Simulated Land Sink

A Representative Concentration Pathway consists of various projected time paths for GHG emissions and concentrations. Each RCP corresponds to an increase, either $+2.6, +4.5, +6.0$ or $+8.5$, in radiative forcing W/m^2 at the end of the 21st century relative to pre-industrial levels. Aggregating by region and sector, an RCP is based on a projected path of carbon factors (carbon per energy unit, kg C/GJ) and energy intensities (energy use per dollar income, GJ/\$) from the present to the end of the century. These projections are in turn generated by distinct integrated assessment models of energy use, fossil fuel emissions, mitigation investments, technological innovations.[14] Lower carbon factor results from input substitution from high carbon emitting sources to lower ones. Lower energy intensity results from combination of technological innovation and conservation efforts.

See van Vuuren et al. (2011)) and the special issue on the RCPs in *Climate Change*, 2011 for an overview and detailed descriptions of each of the RCPs. Table 4 provides a descriptive summary.[15]

Table 4: Summary of RCP Scenarios.

Scenario	Carbon Factor	Energy Intensity
RCP 2.6	Steepest decline reaches lowest steady state	Steepest decline reaches lowest steady state
RCP 4.5	Moderate decline reaches intermediate steady state	Moderate decline reaches intermediate steady state
RCP 6.0	Increase, peak, decline reaches high steady state	Moderate decline reaches intermediate steady state
RCP 8.5	Constant remains at highest steady state	Slow decline reaches highest steady state

The RCP 2.6 achieves the lowest concentrations scenario by 2100. It incorporates a carbon-limiting climate policy and higher rates rates of technological adoption. RCP 8.5 is the highest, assuming higher population growth and slower rates of technological improvement.

[14]Each RCP is based on a separate internally consistent model rather than on distinct parametric assumptions on the same model.

[15]See also van Vuuren et al. (2011), Fig 4).

Using RCP source data from the International Institute for Applied Systems Analysis (IIASA), we construct series on atmospheric stocks $\{g_{t,\,RCP}\}$, fossil fuel emissions $\{\tilde{c}^{fos}_{it,\,RCP}\}$, and capital-emissions ratios $\{H_{it,\,RCP}\}$ as t ranges over quinquennial dates from 2020-2100, and RCP ranges over the four pathways. The atmospheric series $\{g_{t,\,RCP}\}$ are then fed into the estimated absorption equation to produce calibrated values of land sink absorption rates.

The projected values of absorption rates in the active sink model are displayed at the global level in Figure 3. The rates are identical and constant in the constant sink model. Figure 3 displays the global sink absorption rate $\tilde{\rho}_t \equiv \tilde{s}^{lan}_t/\omega^{lan}_{t-1}$ under each of four RCPs from 2020 onward. In three of the four scenarios, absorption ceases and turns negative by the end of the century. In these scenarios, CO2e atmospheric concentrations increase to the end of the century, albeit at decreasing rate for RCP 4.5. Negative values indicate a net *outflow* from land atmospheric carbon. The outflow can occur for a variety of reasons, including stresses from increasing or increasingly volatile temperature, destruction from severe weather events, and impediments to nutrient absorption for high enough CO2 concentrations (Hikosaka et al., 2006; Fernandez-Martinez et al., 2017; Raupach et al., 2014; Feng et al., 2015; Xu, 2015; Zheng et al., 2018). Only in the lowest emissions scenario RCP 2.6 does land sink increase. In this scenario, CO2e concentrations peak early and decline thereafter as strong carbon policies and mitigation technologies take effect. Significantly, the data on growth in GHG concentrations from to 2016 has outpaced the most severe scenarios posited in RCP 8.5.

The paths displayed are roughly consistent in shape though not in levels to forecasts of Thomson et al. (2008) who use the same RCP scenarios. The difference in levels is likely due to the fact that they measure both non-anthropogenic and anthropogenic (e.g., reforestation efforts) contributions to the land sinks. The latter utilizes forecasts of carbon pricing scenarios. Here we look at only non-anthropogenic sink capacity.

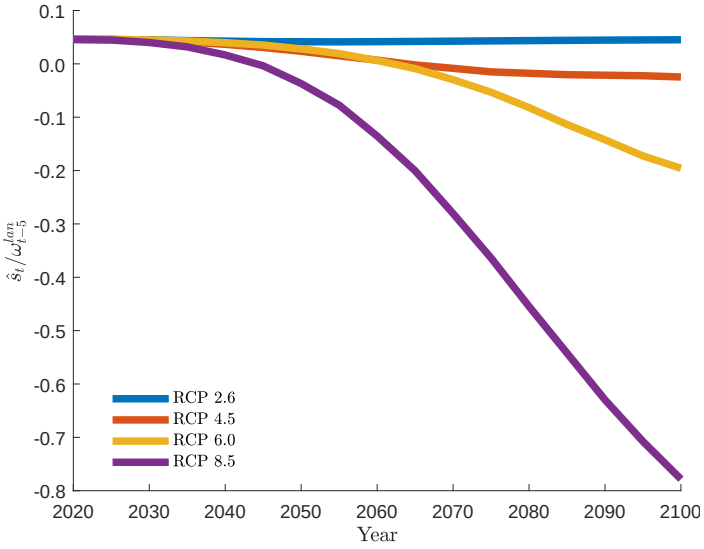

Figure 3: Projected Global (Active) Land Sink Absorption Rates 2020-2100 by IPCC Representative Concentration Pathway.

5.4 Simulated Land Stocks to 2100

The results of Step (ii), the simulation of land carbon stocks for each cluster, each RCP, and in both active and constant sink models are displayed in the panels in Figure 4. Note that by keeping land sink absorption constant, the right-hand side panels are *entirely driven* by simulated forecasts of land use practices. Time paths of carbon stocks therefore do not vary across scenarios.

The graphs in Figure 4 displays the High and Medium high development country clusters in the first row, and Medium Low and Low development clusters in the second. For High and Medium high clusters, land stocks in the active sink model are increasing in the low concentration scenarios RCP 2.6 and 4.5, as is the stock in the constant sink model. There is almost no change between the constant sink model and RCP 2.6. This is due to the fact that the roughly flat trajectory of concentrations in 2.6 will, despite the active sink, appear as if the sink *function* is constant. By contrast, in the high concentration scenarios RCP 6.0 and RCP 8.5, land stocks decline significantly in the active sink model. This is especially true of RCP 8.5. which shows a more than eight-fold decline.

As for Medium Low and Low development clusters, stocks decline in all clusters, RCPs, and sink models. The contrast between high and low development countries

may be due to the fact that mitigation technologies and more sustainable land policies are already in use in the more highly developed countries. As with the higher development clusters, the trajectories of the constant sink and low RCP active sink scenarios are virtually identical, while the declines in the high concentrations and active sink scenarios are dramatic.

Overall, the figures shows that intensive deforestation in the low development countries leads to declines in land stocks. Increased reforestation in high development countries leads to increases in stocks. A final panel, Figure 5, displays the global trajectories in each model.

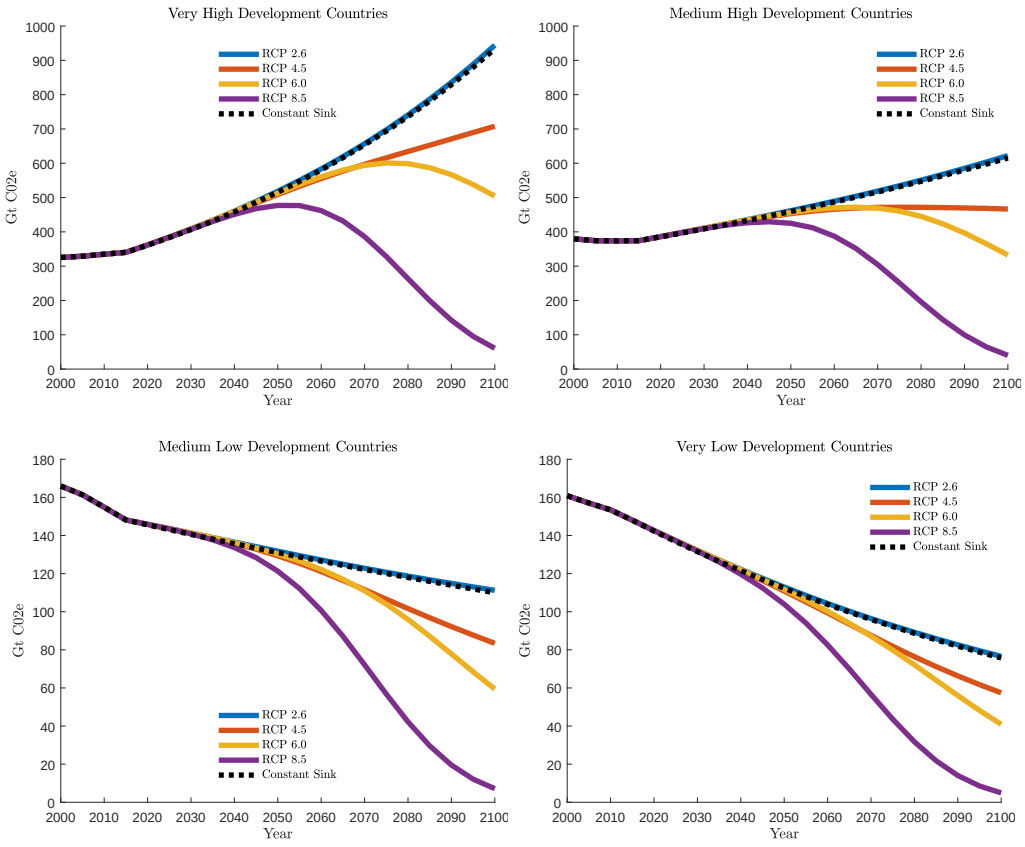

Figure 4: Land Carbon Stocks 2000-2100, by Human Development Index Country Cluster and IPCC Representative Concentration Pathway, Active and Constant Sink.

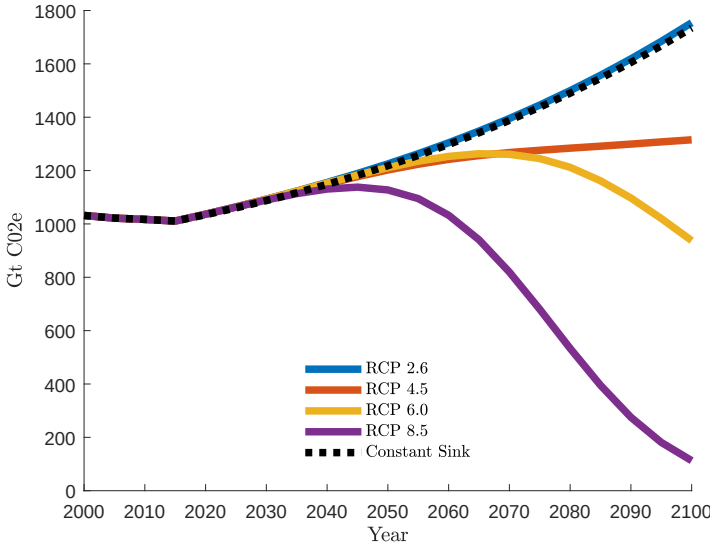

Figure 5: Global Land Carbon Stocks 2000-2100 by IPCC Representative Concentration Pathway, Active and Constant Sink.

5.5 Simulated GDP to 2100

The final step in the exercise simulates GDP to the end of the century in each RCP scenario, for each country, and for each cluster. With the exception of the labor projections $\{L_{it}\}$ which comes from the World Bank and U.N., all forecast data that enter into the GDP simulation are constructed from RCP source data in IIASA and research teams for IPCC's Fifth Assessment Report.[16]

The results are displayed in Figures 6-9. Each figure corresponds to a development cluster. The left-hand panel in each displays the four RCP scenarios in the active sink model (i.e., the Gaussian sink function). The right-hand panel in each displays the four RCP scenarios in the constant sink model Global GDP projections are displayed in Figure 10. Table 5 computes average annual growth rates from 2020 to 2100 for each cluster, scenario, and sink model in our simulation.

Comparing across RCPs in the active sink model. Figures 6-9 indicate that by the end of the century, all clusters exhibit higher GDP in the lower concentrations/emissions scenarios in both active and constant sink models. This is consistent the assumptions underling the RCP emissions paths (van Vuuren et al., 2011). The

[16] Appendix 7.7.

most striking feature is the leveling off and decline of GDP at the higher concentrations scenarios across cluster groups. A stark divergence among the RCPs occurs around mid-century.

The active sink graphs for global GDP in the left-hand panel of Figure 10 displays the sharp contrast between the scenarios. Globally GDP increases 10-fold in RCP 2.6 by the end of the century. This represents an average annual growth rate of 2.7% per year, roughly continuing current growth trends. RCP 4.5 exhibits more moderate, but still positive average annual growth of 1.9%. Global GDP in RCP 6.0 peaks around 2080, then declines somewhat before leveling off in the last decade. Net growth over the next 80 years is less than 1.3% per year. In RCP 8.5, global GDP peaks earlier - around 2060 - and then declines precipitously. Net growth averages out to only 0.6% per year.

Table 5 displays average annual growth rates in GDP in each cluster and scenario, in both the active and constant sink models. As the scenario range from lower to higher GHG concentrations, the average growth differential increases. In the specific clusters the differences in GDP growth between low and high concentrations are largest in the higher development countries. This reflects the higher and more reliable estimates of policy-adjusted elasticities for these countries (Table 2).

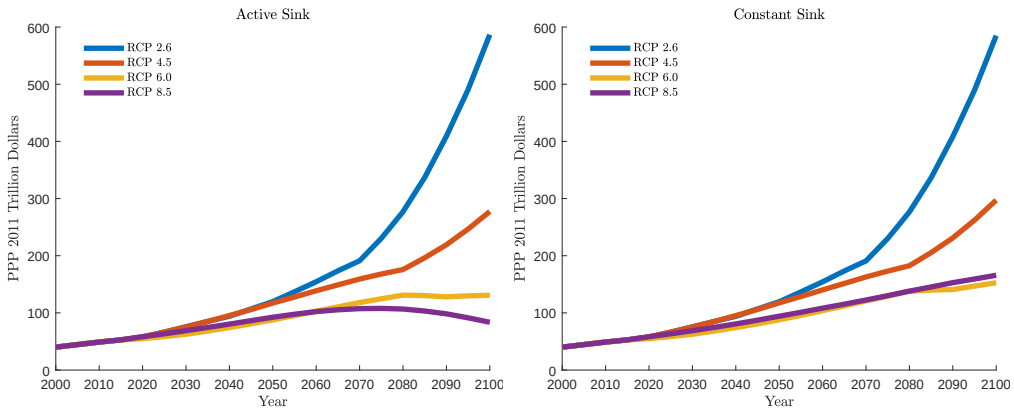

Figure 6: Annual Gross Domestic Product 2000-2100, Very High Development Countries, by IPCC Representative Concentration Pathway, Active and Constant Sink.

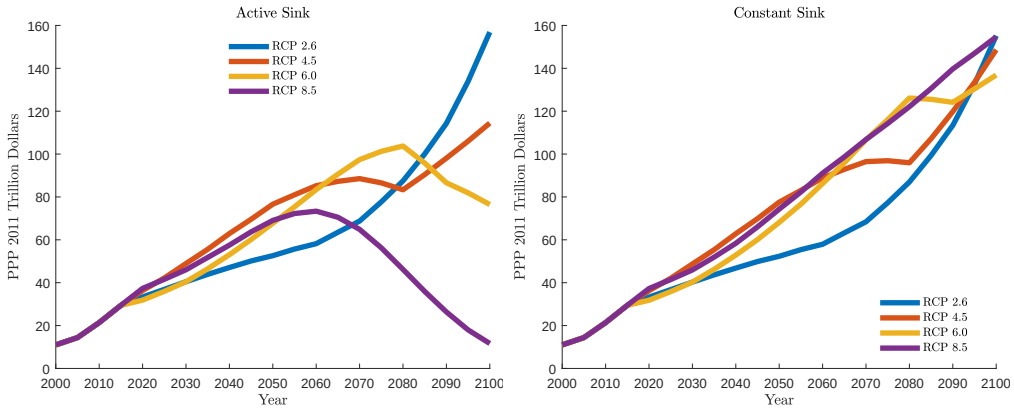

Figure 7: Annual Gross Domestic Product 2000-2100, Medium High Development Countries, by IPCC Representative Concentration Pathway, Active and Constant Sink.

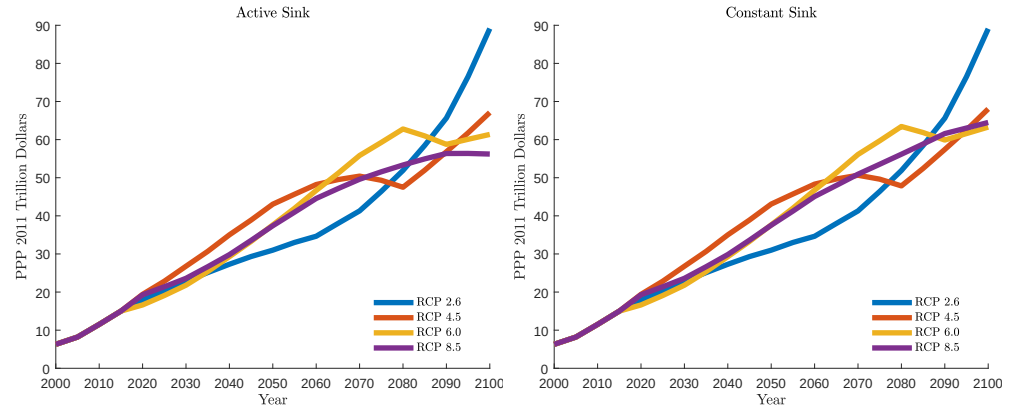

Figure 8: Annual Gross Domestic Product 2000-2100, Medium Low Development Countries, by IPCC Representative Concentration Pathway, Active and Constant Sink.

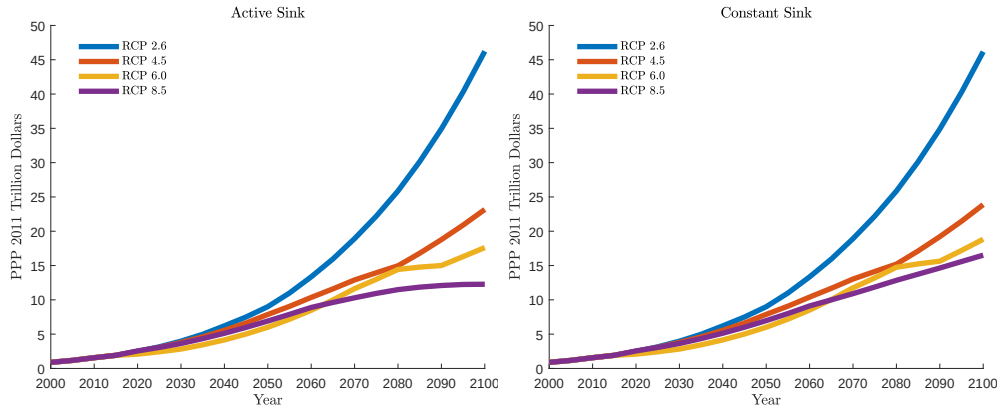

Figure 9: Annual Gross Domestic Product 2000-2100, Very Low Development Countries, by IPCC Representative Concentration Pathway, Active and Constant Sink.

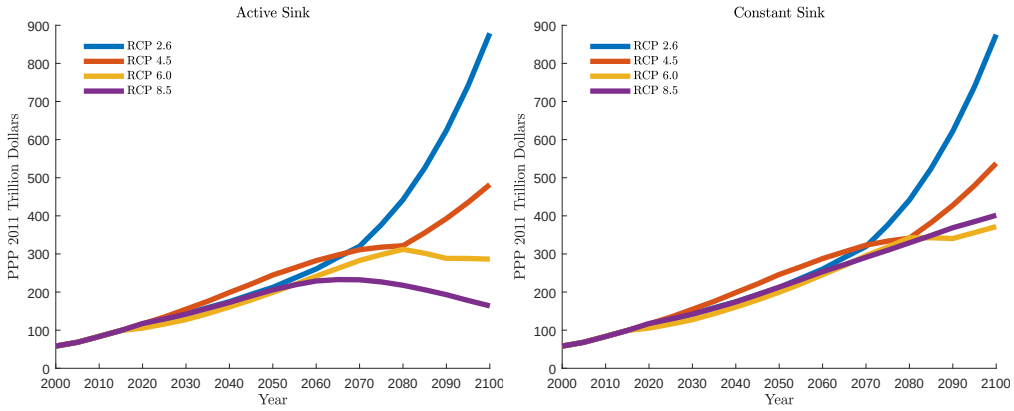

Figure 10: Global Annual Gross Domestic Product 2000-2100, by IPCC Representative Concentration Pathway, Active and Constant Sink.

Table 5: Ave. Annual GDP growth, 2020-2100, Active vs Constant Sink

Active Sink Scenario/HDI cluster	H	MH	ML	L
RCP 2.6	2.9%	2.0%	2.0%	3.7%
RCP 4.5	2.0%	1.4%	1.6 %	2.8%
RCP 6.0	1.1%	1.1%	1.6%	2.7%
RCP 8.5	0.45%	-1.4%	1.3%	2.0%
Constant Sink Scenario/HDI cluster	**H**	**MH**	**ML**	**L**
RCP 2.6	2.9%	1.9%	2.0%	3.7%
RCP 4.5	2.1%	1.8%	1.6 %	2.9%
RCP 6.0	1.3%	1.8%	1.7%	2.8%
RCP 8.5	1.4%	1.8%	1.5%	2.4%

Comparing across sink models.

Comparing the left-hand and right-hand panels in Figures 6-10, one can see the impact of the feedback effects of increasing greenhouse gas concentrations. GDP growth is lower in all but the lowest RCP scenario. By the end of the century, the active sink lowers global GDP by 8% in RCP 4.5, 19% in RCP 6.0, and 60% in RCP 8.5 (Figure 10). The differences are largest in the medium high development countries where sensitivity to declines in carbon stock is highest.

Table 5 displays the comparison in growth rates across the two models. The active sink model displays equal or lower growth rates in all clusters/scenarios. Again, the difference is largest in the medium high development countries and in the highest concentrations scenario.

6 Concluding Remarks

The present paper analyzes a partial equilibrium model of the carbon-based ecosystem. The effect of GHG concentrations on land sink absorption is the key feedback from climate change to GDP in the model. We omit the complexities of the energy market and focus instead on land carbon from a game-theoretic rather than perfect competition perspective.

Naturally, land sink is one among many mechanisms that determine damage from climate change. Even in isolation, its role is subtle. The effects of GHG concentrations on output work both directly and indirectly via endogenous land use.

We are not aware of other models that integrate the effects of non-monotone sink absorption in similar fashion.

Estimated coefficients show that terrestrial carbon stocks, adjusted for equilibrium land use, have potentially large effects on GDP growth, particularly in more highly developed countries. It is unclear why the GDPs of developed countries would be more responsive to land stock changes. One possibility is that interdependencies in more advanced technologies, e.g., computerization of wastewater management systems, are increasingly sensitive to small changes in the ecosystem.

The simulation model is calibrated to the estimated elasticities and parameters of the active land sink absorption function over the 1990-2015 period. We project out from current technological trends to establish an important baseline for future global policies. The results display widely divergent trajectories between RCPs, between developing and developed countries, and between the active and constant sink models. All countries do well under low concentration scenarios. However, the differences between high and low concentration scenarios are greatest for the high and medium high development countries. This may have to do with the relative insensitivity of GDP to land carbon in developing countries and their relatively higher reliance on fossil fuels.

We urge great caution when interpreting the projections. The simulations are based on a specific parametric absorption function. External validation exists for some, but not all, of its attributes. A different approach is taken by Lubowski, Plantinga, and Stavins (2005), who study anthropogenic removals in an econometric model of land use and sinks. Their approach rules out non-monotone absorption rates since sinks are calculated from removals using standard conversion tables (Birdsey, 1992). Hence, their approach is closer to our constant sink model. The studies that validate the active land sink model are regional (e.g., the Hubau et al. (2020) analysis of the Congo), or take place in controlled environments (Xu, 2015). Less is known when CO2 concentrations reach unprecedented levels. This is most relevant for RCP 8.5 scenario in which concentration levels almost triple by 2100.

Not surprisingly, there is considerable controversy about the RCP scenarios themselves. Some claim that RCP 2.6 is all but impossible since the realized path of GHGs has exceeded 2.6 by a wide margin since the scenario was initially published. Others claim that the highest scenario, RCP 8.5, is too extreme to be considered a "business-as-usual" scenario. The present study makes no claim about which, if any, is most likely. By design it utilizes all four. Our intention is to present a broad collection of "possible futures" as a way to facilitate comparisons both across countries and across time.

Finally, the present study focuses exclusively on GDP, a flawed indicator of climate costs. The high growth in output resulting from high emissions scenarios may, in fact, be consistent with poor socio-economic indicators such as lower life expectancy, wellness, and leisure, and increases in congestion, population density, and crime. Even in the context of the model, comparisons are about GDP rather than welfare. The model does not directly measure welfare and so the effects of climate uncertainty are not studied. This simplifies the simulation strategy: the simulations are, effectively, deterministic since shocks enter additively into GDP and wash out in expectation. However, in terms of welfare the volatility of shocks matter a great deal to a representative citizen who values consumption smoothing. In welfare calculations, stochastic simulations that aggregate across payoff paths provide a better indication of true climate costs (see, for instance, (Burke, Hsiang, and Miguel, 2015)). Future work will incorporate broad measures of well being into climate cost scenarios.

References

Acemoglu, D., P. Aghion, L. Bursztyn, and D. Hemous. 2012. "The Environment and Directed Technical Change." *American Economic Review* 102(1):131–166.

Althor, G., J. Watson, and R. Fuller. 2016. "Global Mismatch between Greenhouse Gas Emissions and the Burden of Climate Change." *Scientific Reports* 6(20281).

Birdsey, R.A. 1992. "Carbon Storage and Accumulation in United States Forest Ecosystems." General Technical Report WO-59, U.S.D.A., Forest Service, Washington, DC.

Burke, M., S.M. Hsiang, and E. Miguel. 2015. "Global Non-Linear Effect of Temperature on Economic Production." *Nature* 527:235–39.

Cai, Y., K. Judd, T. Lenton, T. Lontzek, and D. Narita. 2015. "Environmental Tipping Points Significantly Affect the Cost-Benefit Assessment of Climate Policies." *Proceedings of the National Academy of Sciences of the United States of America* 112(15):4606–4611.

Cai, Y., K. Judd, and T. Lontzek. 2012. "Tipping Points in a Dynamic Stochastic IAM." Working Paper 12-13, Robust Decision-making on Climate and Energy Policy, Chicago, IL.

Calel, Raphael and David A. Stainforth. 2017. "On the Physics of Three Integrated Assessment Models." *Bulletin of the American Meteorological Society* 98(6):1199–1216. URL `https://doi.org/10.1175/BAMS-D-16-0034.1`.

Canadell, J., C. Le Quere, M. Raupach, C. Field, E. Buitenhuis, P. Ciais, T. Conway, N. Gillett, R. A. Houghton, and G. Marland. 2007. "Contributions to Accelerating Atmospheric CO2 Growth from Economic Activity, Carbon Intensity, and Efficiency of Natural Sinks." *Proceedings of the National Academy of Sciences of the United States of America* 104(47):18866–18870.

Cave, J. 1987. "Long-Term Competition in a Dynamic Game: The Cold Fish War." *Rand Journal* 18(4):596–610.

Clarke, L., J. Edmonds, H. Jacoby, H. Pitcher, J. Reilly, and R. Richels. 2007. "Scenarios of Greenhouse Gas Emissions and Atmospheric Concentrations." Tech. rep., U.S. Climate Change Science Program and the Subcommittee on Global Change Research. Department of Energy, Office of Biological and Environmental Research, Washington, DC.

Dell, M., B. Jones, and B. Olken. 2012. "Temperature Shocks and Economic Growth: Evidence from the Last Half Century." *American Economic Journal: Macroeconomics* 4(3):66–95.

Deryugina, T. and S. Hsiang. 2017. "The Marginal Product of Climate." Working Paper 24072, National Bureau of Economic Research, Cambridge, MA.

Dutta, P. and R. Radner. 2004. "Self-Enforcing Climate-Change Treaties." *Proceedings of the National Academy of Sciences of the United States of America* 101(14):5174–5179.

———. 2006. "A Game-Theoretic Approach to Global Warming." In *Advances in Mathematical Economics, Volume 8*, edited by S. Kusuoka and A. Yamazaki. Tokyo, Japan: Springer, 135–153.

———. 2009. "A Strategic Analysis of Global Warming: Theory and Some Numbers." *Journal of Economic Behavior and Organization* 71(2):187–209.

FAO. 2015. "Forest Resources Assessment." Report, Food and Agricultural Organization of the United Nations, Rome, Italy.

———. 2019. "FAOSTAT." Accessible at www.fao.org/faostat/en/.

Feng, Z., T. Rutting, H. Pleijel, G. Wallin, P. Reich, C. Kamnann, P. Newton, K. Kobayashi, Y. Luo, and J. Udding. 2015. "Constraints to Nitrogen Acquisition of Terrestrial Plants under Elevated CO2." *Global Change Biology* 21(8):3152–3168.

Fernandez-Martinez, M., S. Vicca, I. Janssens, P. Ciais, M. Obersteiner, M. Bartrons, J. Sardans, A. Verger, J.G. Canadell, F. Chevallier, X. Wang, C. Bernhofer, P.S. Curtis, D. Gianelle, T. Grünwald, B. Heinesch, A. Ibrom, A. Knohl, T. Laurila, B. Law, J. Limousin, B. Longdoz, D. Loustau, I. Mammarella, G. Matteucci, R. Monson, L. Montagnani, E. Moors, J. Munger, D. Papale, S. Piao, and J. Pe nuelas. 2017. "Atmospheric Deposition, CO2, and Change in the Land Carbon Sink." *Scientific Reports* 7(1):9632.

Fisher, R. and L. Mirman. 1992. "Strategic Dynamic Interactions: Fish Wars." *Journal of Economic Dynamics and Control* 16(2):267–287.

Fujino, J., R. Nair, M. Kainuma, T. Masui, and Y. Matsuoka. 2006. "Multi-Gas Mitigation Analysis on Stabilization Scenarios Using AIM Global Model: Multigas Mitigation and Climate Policy." *The Energy Journal* 27(3):343–354.

Golosov, M., J. Hassler, P. Krusell, and A. Tsyvinski. 2014. "Optimal Taxes on Fossil Fuel in General Equilibrium." *Econometrica* 82(1):41–88.

Golub, A., T. Hertel, and B. Sohngen. 2008. "Land Use Modeling in Recursively-Dynamic GTAP Framework." *GTAP Working Paper 48* .

Harrison, R. and R. Lagunoff. 2017. "Dynamic Mechanism Design for a Global Commons." *International Economic Review* 58(3):751–782.

———. 2019. "Tipping Points and Business-as-Usual in a Global Commons." *Journal of Economic Behavior and Organization* 163(July):386–408.

Hassler, J. and P. Krusell. 2018. "Environmental Macroeconomics: the Case of Climate Change." *Handbook of Macroeconomics* 8:333–394.

Hijioka, Y., Y. Matsuoka, H. Nishimoto, M. Masui, and M. Kainuma. 2008. "Global GHG Concentration Scenarios under GHG Concentration Stabilization Targets." *Journal of Global Environmental Engineering* 13:97–108.

Hikosaka, K., I. Kazumasa, A. Borjigidai, O. Muller, and Y. Onoda. 2006. "Temperature Acclimation of Photosynthesis: Mechanisms Involved in the Changes

in Temperature Dependence of Photosynthetic Rate." *Journal of Experimental Botany* 57(2):291–302.

Hsiang, S., R. Kopp, A. Jina, J. Rising, M. Delgado, S. Mohan, D.J. Rasmussen, R. Muir-Wood, P. Wilson, M. Oppenheimer, K. Larsen, and T. Houser. 2017. "Estimating Economic Damage from Climate Change in the United States." *Science* 356(6345):1362–1369.

Hubau, W., S.L. Lewis, O.L. Phillips, and et al. 2020. "Asynchronous carbon sink saturation in African and Amazonian tropical forests." *Nature* 579:80–87.

IPCC. 2014. "Fifth Assessment Report on Climate Change." Technical report, Inter-Governmental Panel on Climate Change, Geneva, Switzerland.

Ito, A.J., M. Penner, C. Prather, C. de Campos, R.A. Houghton, T. Kato, A. Jain, X. Yang, G. Hurtt, S. Frolking, M. Fearon, L. Chini, A. Wang, and D. Price. 2008. "Can We Reconcile Differences in Estimates of Carbon Fluxes from Land-Use Change and Forestry for the 1990s?" *Atmospheric Chemistry and Physics* 8(12):3291–3310.

Le Quere, C., R. Andrew, R. M., Friedlingstein, P., Sitch, S., Hauck, J., Pongratz, J., Pickers, P. A., Korsbakken, J. I., Peters, G. P., Canadell, J. G., Arneth, A., Arora, V. K., Barbero, L., Bastos, A., Bopp, L., Chevallier, F., Chini, L. P., Ciais, P., Doney, S. C., Gkritzalis, T., Goll, D. S., Harris, I., Haverd, V., Hoffman, F. M., Hoppema, M., Houghton, R. A., Hurtt, G., Ilyina, T., Jain, A. K., Johannessen, T., Jones, C. D., Kato, E., Keeling, R. F., Goldewijk, K. K., Landschützer, P., Lefèvre, N., Lienert, S., Liu, Z., Lombardozzi, D., Metzl, N., Munro, D. R., Nabel, J. E. M. S., Nakaoka, S.-I., Neill, C., Olsen, A., Ono, T., Patra, P., Peregon, A., Peters, W., Peylin, P., Pfeil, B., Pierrot, D., Poulter, B., Rehder, G., Resplandy, L., Robertson, E., Rocher, M., Rödenbeck, C., Schuster, U., Schwinger, J., Séférian, R., Skjelvan, I., Steinhoff, T., Sutton, A., Tans, P. P., Tian, H., Tilbrook, B., Tubiello, F. N., van der Laan-Luijkx, I. T., van der Werf, G. R., Viovy, N., Walker, A. P., Wiltshire, A. J., Wright, R., Zaehle, S., Zheng, and B. 2018. "Global Carbon Budget 2018." *Earth Systems Science Data* 10(4):2141–2194.

Levhari, D. and L. Mirman. 1980. "The Great Fish War: An Example Using a Dynamic Cournot-Nash Solution." *Bell Journal of Economics* 14(1):322–334.

Lubowski, R.N., A Plantinga, and R. Stavins. 2005. "Land-Use Change and Carbon Sinks: Econometric Estimation of the Carbon Sequestration Supply Function." *Journal of Environmental Economics and Management* 51(2):135–152.

Mcalpine, K.G. and D.M. Wotton. 2009. "Conservation and the Delivery of Ecosystem Services: A Literature Review." Science for Conversation Report 295, New Zealand Department of Conservation, Wellington, New Zealand.

Meinshausen, M., S. C. B. Raper, and T. M. L. Wigley. 2011. "Emulating coupled atmosphere-ocean and carbon cycle models with a simpler model, MAGICC6 Part 1: Model description and calibration." *Atmospheric Chemistry and Physics* 11(4):1417–1456. URL `https://www.atmos-chem-phys.net/11/1417/2011/`.

Mooney, C. and Z. Murphy. 2019. "Gone in a Generation." January 29, 2019. Accessible at www.washingtonpost.com/graphics/2019/national/gone-in-a-generation/?noredirect=on.

Narayan, S., M. Beck, P. Wilson, C. Thomas, A. Guerrero, C. Shepard, B. Reguero, G. Franco, J. Ingram, and D. Trespalacios. 2017. "The Value of Coastal Wetlands for Flood Reduction in the Northeastern USA." *Scientific Reports* 7(1):9643.

Nordhaus, W. 2014. "Estimates of the Social Costs of Carbon: Concepts and Results from the DICE-2013R Model and Alternative Approaches." *Journal of the Association of Environmental and Resource Economists* 1(1/2):273–312.

———. 2018. "Projections and Uncertainties about Climate Change in an Era of Minimal Climate Policies." *American Economic Journal: Economic Policy* 10(3):333–360.

Nordhaus, W. and A. Moffat. 2017. "A Survey of Global Impacts of Climate Change: Replication Survey Methods, and a Statistical Analysis." Working Paper 23646, National Bureau of Economic Research, Cambridge, MA.

Power, A. 2010. "Ecosystem Services and Agriculture: Tradeoffs and Synergies." *Philosophical Transactions of the Royal Society B* 365(1554):2959–2571.

Raupach, M.R., M. Gloor, J.L. Sarmiento, J.G. Canadell, T.L. Fralicher, T. Gasser, R.A. Houghton, C. Le Quere, and C.M. Trudinger. 2014. "The Declining Uptake Rate of Atmospheric CO2 by Land and Ocean Sinks." *Biogeosciences* 11(13):3453–3475.

Riahi, K. and N. Nakicenovic. 2007. "Greenhouse Gases - Integrated Assessment." *Technological Forecasting and Social Change* 74(7):873–1108.

Rights and Resources Initiative. 2015. "Who Owns the World's Land? A Global Baseline of Normally Recognized Indigenous and Community Land Rights." Tech. rep., Rights and Resources Group, Washington, DC.

Smith, S.J. and T.M.L. Wigley. 2006. "Multi-Gas Forcing Stabilization with the MiniCAM." *The Energy Journal* 27:373–391.

Thomson, A., R. Izaurralde, S. Smith, and L. Clarke. 2008. "Integrated Estimates of Global Terrestrial Carbon Sequestration." *Global Environmental Change* 18(1):192–203.

Tol, R. 2009. "The Economic Effects of Climate Change." *Journal of Economic Perspectives* 23(12):29–51.

United Nations Development Programme. 2019. "Human Development Reports." Accessible at www.hdr.undp.org.

van Vuuren, D.P., M. den Elzen, P. Lucas, B. Eickhout, B. Strengers, B. van Ruijven, and S. Wonink andand R. van Houdt. 2007. "Stabilizing Greenhouse Gas Concentrations At Low Levels: An Assessment of Reduction Strategies and Costs." *Climatic Change* 81(2):119–159.

van Vuuren, D.P., J. Edmonds, M. Kainuma, K. Riahi, A. Thomson, K. Hibbard, G.C. Hurtt, T. Kram, V. Krey, J.F. Lemarque, T. Matsui, M. Meinhausen, N. Nakicenovic, S. Smith, and A. Rose. 2011. "The Representative Concentration Pathways: an Overview." *Climatic Change* 109(1):5–31.

van Vuuren, D.P., B. Eickhout, P.L. Lucas, and M.G.J. den Elzen. 2006. "Long-Term Multi-Gas Scenarios To Stabilise Radiative Forcing — Exploring Costs and Benefits within an Integrated Assessment Framework: Multigas Mitigation and Climate Policy." *The Energy Journal* 27(1):201–234.

Vincent, C.H., L.A. Hanson, and C.N. Argueta. 2017. "Federal Land Ownership: Overview and Data." Tech. rep., Congressional Research Service, Washington, DC.

Wise, M.A., K.V. Calvin, A.M. Thomson, L.E. Clarke, B. Bond-Lamberty, R.D. Sands, S.J. Smith, A.C. Janetos, and J.A. Edmonds. 2009. "Implications of Limiting CO2 Concentrations for Land Use and Energy." *Science* 324(5931):1183–1186.

Xu, M.N. 2015. "The Optimal Atmospheric CO2 Concentration for the Growth of Winter Wheat (Triticum Aestivum)." *Journal of Plant Physiology* 184(July):89–97.

Zheng, Y., F. Li, A.A. Shedayi, L. Guo, C. Ma, B. Huang, and M. Xu. 2018. "The Optimal CO2 Concentrations for the Growth of Three Grass Species." *BMC Plant Biology* 18(1):27.

Zomer, R.J., H. Neufeldt, J. Xu, A. Ahrends, D. Bossio, A. Trabucco, M. van Noordwijk, and M. Wang. 2016. "Global Tree Cover and Biomass Carbon on Agricultural Land: The Contribution of Agroforestry to Global and National Carbon Budgets." *Scientific Reports* 6:29987.

7 Appendix

7.1 Derivation of the Equilibrium Land Use Policies

Due to additively separability under log payoffs, we can drop the noise term ϵ_{yit} and the terms H_{it}, c_{it}^{fos} and L_{it} from the derivation of equilibrium land policy for country i. As these are not determined by the land-policy maker, none of these terms enter into i's land-policy function.

Consequently, we also drop the "lan" superscript and the country subscript " i" from land consumption c_{it}^{lan}, removals r_{it}^{lan}, land stock ω_{it}^{lan}, and land sink s_{it}^{lan}.

Dropping these terms, the structural equations are expressed as

$$u_t = \log(y_t) + \theta \log(\omega_{t-1} - r_t) \tag{27}$$

$$y_t = A c_t^{\alpha} (\omega_{t-1} + s_t + r_t - c_t)^{\beta} \tag{28}$$

$$\omega_t = \omega_{t-1} + s_t + r_t - c_t \tag{29}$$

Now let

$$s_t \equiv \ell_t \omega_{t-1},\ r_t \equiv q_t \omega_{t-1},\ c_t \equiv e_t \omega_{t-1}, \tag{30}$$

The rates ℓ_t, q_t, and e_t can potentially vary with t.

By equations (29) and (30),

$$\omega_t = \omega_{t-1}(1 + \ell_t + q_t - e_t) \tag{31}$$

Given the notation above, the Bellman equation is

$$\begin{aligned} U_t(\omega_{t-1}) = \max_{e,t,q_t} \ & \{\alpha \log(e_t) + \beta \log(1 + q_t + \ell_t - e_t\ ) + \theta \log(1 - q_t) \\ & + (\alpha + \beta + \theta) \log(\omega_{t-1}) + \delta\ U_{t+1}(\omega_t)\} \end{aligned} \tag{32}$$

7.1.1 Derivation of equilibrium Land Carbon Emissions Rate e_t

The first order condition in e_i is

$$\frac{\alpha}{e_t} - \frac{\beta}{1 + \ell_t + q_t - e_t} = \delta \frac{\partial U}{\partial \omega_t} \omega_{t-1} \tag{33}$$

Differentiating the value function,

$$\begin{aligned}\frac{\partial U}{\partial \omega_t} &= \frac{\alpha+\beta+\theta}{\omega_t} + \delta\frac{\partial U}{\partial \omega_{t+1}}(1+\ell_{t+1}+q_{t+1}-e_{t+1})) \\ &= \frac{\alpha+\beta+\theta}{\omega_t} + \left(\frac{\alpha}{e_{t+1}} - \frac{\beta}{1+\ell_{t+1}+q_{t+1}-e_{t+1}}\right)\frac{1}{\omega_t}(1+\ell_{t+1}+q_{t+1}-e_{t+1}) \\ &\quad \text{(second equality is from substituting FOC one period forward.)}\end{aligned} \tag{34}$$

Substituting (34) into the FOC (33), we obtain

$$\begin{aligned}&\frac{\alpha}{e_t} - \frac{\beta}{1+\ell_t+q_t-e_t} \\ &= \delta\frac{\omega_{t-1}}{\omega_t}\left[(\alpha+\beta+\theta) + \left(\frac{\alpha}{e_{t+1}} - \frac{\beta}{1+\ell_{t+1}+q_{t+1}-e_{t+1}}\right)(1+\ell_{t+1}+q_{t+1}-e_{t+1})\right] \\ &= \frac{\delta\omega_{t-1}}{\omega_{t-1}(1+\ell_t+q_t-e_t)}\left[(\alpha+\beta+\theta) + \left(\frac{\alpha}{e_{t+1}} - \frac{\beta}{1+\ell_{t+1}+-e_{t+1}}\right)(1+\ell_{t+1}+q_{t+1}-e_{t+1})\right]\end{aligned} \tag{35}$$

or

$$\frac{\alpha(1+\ell_t+q_t-e_t)}{e_t} - \beta = \delta\left[(\alpha+\beta+\theta)\left(\frac{\alpha(1+\ell_{t+1}+q_{t+1}-e_{t+1})}{e_{t+1}} - \beta\right)\right] \tag{36}$$

Iterating forward yields

$$\frac{\alpha(1+\ell_t+q_t-e_t)}{e_t} - \beta = \frac{\delta}{1-\delta}(\alpha+\beta+\theta) \tag{37}$$

Solving for e_t yields

$$e_t = \frac{\alpha(1-\delta)(1+\ell_t+q_t)}{(1-\delta)(\alpha+\beta)+\delta(\alpha+\beta+\theta)\theta)} \tag{38}$$

We are not yet done since q_t is also an endogenous choice by the country.

7.1.2 Derivation of equilibrium Land Carbon Removals Rate q_t

The first order condition in q_t is

$$-\frac{\theta}{1-q_t} + \frac{\beta}{1+\ell_t+q_t-e_t} + \delta\frac{\partial U}{\partial \omega_t}\omega_{t-1} = 0 \tag{39}$$

which we can rewrite as

$$\frac{\theta}{1-q_t} - \frac{\beta}{1+\ell_t+q_t-e_t} = \delta \frac{\partial U}{\partial \omega_t}\omega_{t-1} \tag{40}$$

Once more we differentiate the value function,

$$\begin{aligned}\frac{\partial U}{\partial \omega_t} &= \frac{\alpha+\beta+\theta}{\omega_t} + \delta \frac{\partial U}{\partial \omega_{t+1}}(1+\ell_{t+1}+q_{t+1}-e_{t+1})) \\ &= \frac{\alpha+\beta+\theta}{\omega_t} + \left(\frac{\theta}{1-q_{t+1}} - \frac{\beta}{1+\ell_{t+1}+q_{t+1}-e_{t+1}}\right)\frac{1}{\omega_t}(1+\ell_{t+1}+q_{t+1}-e_{t+1}) \\ &\quad \text{(second equality is from substituting FOC one period forward.)}\end{aligned} \tag{41}$$

Substituting (41) into the FOC (40), we obtain

$$\begin{aligned}&\frac{\theta}{1-q_t} - \frac{\beta}{1+\ell_t+q_t-e_t} \\ &= \delta\frac{\omega_{t-1}}{\omega_t}\left[(\alpha+\beta+\theta) + \left(\frac{\theta}{1-q_{t+1}} - \frac{\beta}{1+\ell_{t+1}+q_{t+1}-e_{t+1}}\right)(1+\ell_{t+1}+q_{t+1}-e_{t+1})\right] \\ &= \frac{\delta\omega_{t-1}}{\omega_{t-1}(1+\ell_t+q_t-e_t)}\left[(\alpha+\beta+\theta) + \left(\frac{\theta}{1-q_{t+1}} - \frac{\beta}{1+\ell_{t+1}+-e_{t+1}}\right)(1+\ell_{t+1}+q_{t+1}-e_{t+1})\right]\end{aligned} \tag{42}$$

or

$$\frac{\theta(1+\ell_t+q_t-e_t)}{1-q_t} - \beta = \delta\left[(\alpha+\beta+\theta)\left(\frac{\theta(1+\ell_{t+1}+q_{t+1}-e_{t+1})}{1-q_{t+1}} - \beta\right)\right] \tag{43}$$

Iterating forward yields

$$\frac{\theta(1+\ell_t+q_t-e_t)}{1-q_t} - \beta = \frac{\delta}{1-\delta}(\alpha+\beta+\theta) \tag{44}$$

Notice that this looks a lot like Equation (37). Since the right-hand side of (37) and (44) are the same, we equate the left hand sides to obtain

$$q_t = 1 - \frac{\theta}{\alpha}e_t \tag{45}$$

This is an easy equation that relates the equilibrium choices of q_t and e_t. Substituting (45) into the equation (38) we obtain

$$e_t = \frac{\alpha(1-\delta)(1+\ell_t+(1-\frac{\theta}{\alpha}e_t))}{(1-\delta)(\alpha+\beta)+\delta(\alpha+\beta+\theta)} \tag{46}$$

Solving for e_t (with a few steps of algebra) we obtain the equilibrium rate of land carbon extraction

$$e_t^* = \frac{\alpha(1-\delta)(2+\ell_t)}{\alpha+\beta+\theta} \tag{47}$$

Finally, substituting (47) into the equation for q_t, i.e., $q_t = 1 - \frac{\theta}{\alpha}e_t$ from (45) we obtain he equilibrium rate of atmospheric removal:

$$q_t^* = 1 - \frac{\theta(1-\delta)(2+\ell_t)}{\alpha+\beta+\theta} \tag{48}$$

Multiplying e_t^* and q_t^* by ω_{t-1}^{lan} gives the resulting equilibrium consumption and removal policies, c_t^* and r_t^*, respectively.

Multiplying both sides of (47) and (48) by the state ω_{t-1}, we we obtain

$$\begin{aligned} c_t^* &= \frac{\alpha(1-\delta)(2\omega_{t-1}+s_t)}{\alpha+\beta+\theta} \quad \text{and} \\ r_t^* &= \omega_{t-1} - \frac{\theta(1-\delta)(2\omega_{t-1}+s_t)}{\alpha+\beta+\theta} \end{aligned} \tag{49}$$

7.2 Estimating Equation

We show how the equilibrium choices in (49) can generate a simple estimating equation.

Substitute the functions in (49) into the law of motion. This yields

$$\begin{aligned} \omega_t &= \omega_{t-1} + s_t + r_t^* - c_t^* \\ &= \left(1 - \frac{(1-\delta)(\alpha+\theta)}{\alpha+\beta+\theta}\right)(2\omega_{t-1}+s_t) \end{aligned} \tag{50}$$

Notice that one can separate out the term $2\omega_{t-1} + s_t$ from the parameters. Our estimating equation in logs, ignoring the scale term A_i, and fossil fuel c_{it}^{fos}, capital-emissions H_{it}, and labor L_t, is

$$\log(y_t) = \alpha \log\left(\frac{\alpha(1-\delta)}{\alpha+\beta+\theta}\right) + \beta \log\left(1 - \frac{(1-\delta)(\alpha+\theta)}{\alpha+\beta+\theta}\right) + (\alpha+\beta)\log\left(2\omega_{t-1} + s_t\right) \tag{51}$$

So the first two terms on the right-hand side are constants. The second term has the same coefficient, $\alpha+\beta$ as before, and the data is $2\omega_{t-1}+s_t$ each period. Equation (51) coincides with Equation (11) once the other variables, H_{it}, c_{it}^{fos} and L_{it} and the error ϵ_{it} are added back. Notice that separate data series for individual consumption c_t and removals r_t are not needed to estimate Equation (11).

7.3 Units of Measurement

- *CO2e.* Units of CO2e convert all green house gases (CH4 Methane, CO2 Carbon Dioxide, N2O Nitrous Oxide, and three fluorinated gases: Hydrofluorocarbons, Perfluorocarbons, and Sulfur Hexafluoride) into CO2 by measuring Global Warming Potential (GWP), a relative measure of how much heat a greenhouse gas traps in the atmosphere. It compares the "amount of heat trapped by a certain mass of the gas in question to the amount of heat trapped by a similar mass of carbon dioxide."

- *Conversion factors.* 1 PPM CO2e = 7.81 Gt CO2e. 1 Gt C = 3.67 Gt C02e

- *Date t index and Period Length.* The date "t" indexes quinquennial dates $1990, 1995, \ldots, 2015$ while "τ" indexes annual dates, $1990, 1991, 1992, \ldots, \ldots, 2015$. In all the series below, a length of time is five years (though for some purposes, annual rolling five year aggregates are used). Flow data is a five year aggregated flow. Stock data is the value given in the particular year. Data used in the input file consists of stock data in the years at the end of a quinquennial time period t (e.g., stock data for the period 1991-1995 is the stock year 1995), and flow data ending in 1995 that aggregates the annual flows in a quinquennial time period, e.g., the yearly flows from 1991 to 1995.[17]

[17]FAOSTAT data conforms to U.N. reporting requirements of five year increments, each date t represents the end of a five year period up to and including the current year. In particular, the

- *Country Index i.* Country index i ranges over 152 countries that are included in at at least one cluster: Albania, Algeria, Angola, Argentina, Armenia, Australia, Austria, Azerbaijan, Bahamas, Bahrain, Bangladesh, Barbados, Belarus, Belgium, Belize, Benin, Bhutan, Bolivia, Bosnia and Herzegovina, Botswana, Brazil, Brunei Darussalam, Bulgaria, Burkina Faso, Burundi, Cabo Verde, Cambodia, Cameroon, Canada, Central African Republic, Chad, Chile, China, Colombia, Comoros, Congo, Dem. Republic Congo, Costa Rica, Cote d'Ivoire, Croatia, Cyprus, Czech Republic, Denmark, Dominican Republic, Ecuador, Egypt, El Salvador, Equatorial Guinea, Estonia, Ethiopia, Fiji, Finland, France, Gabon, Gambia, Georgia, Germany, Ghana, Greece, Guatemala, Guinea, Guinea-Bissau, Honduras, Hungary, Iceland, India, Indonesia, Iran, Iraq, Ireland, Israel, Italy, Jamaica, Japan, Jordan, Kazakhstan, Kenya, Korea, Rep., Kuwait, Kyrgyzstan, Laos, Latvia, Lebanon, Lesotho, Lithuania, Macedonia FYR, Madagascar, Malawi, Malaysia, Mali, Malta, Mauritania, Mauritius, Mexico, Moldova, Mongolia, Morocco, Mozambique, Myanmar, Namibia, Nepal, Netherlands, New Zealand, Nicaragua, Niger, Nigeria, Norway, Oman, Pakistan, Panama, Paraguay, Peru, Philippines, Poland, Portugal, Romania, Russia, Rwanda, Saint Lucia, Saint Vincent and the Grenadines, Saudi Arabia, Senegal, Serbia, Sierra Leone, Singapore, Slovakia, Slovenia, South Africa, Spain, Sri Lanka, Sudan, Suriname, Sweden, Switzerland, Tajikistan, Thailand, Togo, Trinidad and Tobago, Tunisia, Turkey, Turkmenistan, Uganda, Ukraine, United Arab Emirates, United Kingdom United States of America, Uruguay, Uzbekistan, Venezuela, Viet Nam, Zambia, Zimbabwe.

7.4 Description of the Historical Data

- *Global land sink*: The data on global annual sink s_τ^{lan} comes from the Global Carbon Project 2018 (GCP 2018). GCP 2018 data is annual. The sink s_τ^{lan} (with τ representing a period of a year) is "estimated by the difference of the other terms of the global carbon budget and compared to results of independent Dynamic Global Vegetation Models forced by observed climate, CO2 and land cover change (some including nitrogen-carbon interactions)..."[18] The data used in for our estimation are five year flows up to and including τ so that $\tilde{s}_\tau^{lan} =$

UNCCC reporting procedures require countries to update their carbon measurement every 5 years, typically in years ending in 0 or 5. measurements typically occur in years 1990, 2000, 2005, 2010, and 2015. While FAOSTAT does report annual data, the data in the intervening years appears to be extrapolated from the quinquennial reports.

[18] Le Quere et al. (2016), p. 3.

$\sum_{j=0}^{4} s_{\tau-j}$. Annual data on 5-year rolling aggregates is needed to obtain large enough sample sizes for estimation (see Appendix 7.6 for details).

- *Global land carbon stock*: The global land stock data is annual from 1982 to 2015. The series for ω_{τ}^{lan} is then constructed from a benchmark value set at FAO Forest Carbon stock in the base year 1990. Additions and subtractions from the base year are then determined annually by land emissions (land use − land sink) series from GCP 2018 (the same source used for s_t^{lan}), dating back to 1982. Net land emissions are subtracted forward and added backward from the base year to obtain an annual series from 1982 to 2015. The annual data is used for constructing the 5 year rolling aggregate $\tilde{s}_{\tau}^{lan}, \omega_{\tau-5}^{lan}$ land sink rate as τ varies annually from 1990-2015.[19]

- *Country land carbon stocks*: FAOSTAT contains data on Forest Carbon stock in living (above and below ground) biomass for each country and derived from the FAO Forest Resource Assessments (FAO FRA). The data measures only living biomass in forests. See http://www.fao.org/faostat/en/#data.[20] FAOSTAT data is updated at quinquennial intervals from 1990 to 2015. The annual data in the interim years reported by FAOSTAT is interpolated. Interpolated is not used in our study.

- *Country land sinks*: The model posits absorption efficiency per unit land carbon biomass to be identical across all country's stocks, global land sink data is used to compute country-specific sinks per unit carbon biomass. Specifically, for quinquennial dates t, $\frac{\tilde{s}_{it}^{lan}}{\omega_{it-5}^{lan}} = \frac{\tilde{s}_{t}^{lan}}{\omega_{it-5}^{lan}}$. With the data on land stocks and on the global sinks, the country specific land sink $\tilde{s}_{it}^{lan}$ is constructed.

- *Global atmospheric GHG stock*: Annual data on global GHG atmospheric (CO2e) stocks g_t from 1982 to 2016 are taken from NOAA Earth Systems

[19]The FAO series "forest carbon stocks" is inadequate. It interpolates between five year periods from 1990 to 2015 and so has six distinct data points. The constructed series by contrast is annual data from 1982-2015.

[20]Data on soils, leaf litter is found in FAO's Global Forest Resource Assessment 2015 for the single year 2015. Data on biomass on agricultural land is found in Zomer et al. (2016) for the years 2000 and 2010. Forest biomass is significantly larger than agricultural biomass in most countries. In 2010 in the U.S. the agricultural carbon stock is 9.5% of the total. In Brazil, 11.5%. In India, however, agricultural biomass is 41%. Agricultural carbon stock is excluded since data from Zomer et al. (2016) only covers two years, 2000 and 2010. In the U.S. agricultural stock was measured by Zomer to be 6.34 GtCO2e in 2000 and 6.62 Gt CO2e in 2010. Forestry stock in those two years measured measured 57.66 and 62.64 in those years, resp. Hence agricultural stock comprised 10% and 9.5% of the total carbon stocks in those years.

Research Laboratory. The NOAA report is a time series of atmospheric CO2e levels from the Moana Loa Observatory. Data is expressed in parts per million by volume (ppm). To convert from ppm to gigatonne of carbon, the conversion tables of the Carbon Dioxide Information Analysis Center advise that 1 part per million of atmospheric CO2e is equivalent to 7.81 Gt CO2e. The GHG concentrations include non-carbon GHGs contributing to temperature rises that determine land sink absorption rate. The index t is over quinquennial dates.

- *Country fossil fuel emissions*: Annual data on fossil fuel consumption $c_{i\,\tau}^{fos}$ for each country is from the CAIT Climate Data Explorer, 2017, the database provided by the World Resources Institute, http://cait.wri.org/historical. From this data we construct five year flows for our estimation: $\tilde{c}_{it}^{fos}$ is the five year sum: $\tilde{c}_{it}^{fos} = \sum_{j=0}^{4} c_{i,\,\tau-j}^{fos}$.

- *Country output and labor*: Annual GDP $y_{i\,\tau}$ and labor $L_{i\,\tau}$ series are taken from the World Bank database. GDP is in 2011 PPP constant dollars. From this data we construct five year flows for output: $\tilde{y}_{it} = \sum_{j=0}^{4} y_{i,\,\tau-j}$. Labor is a stock variable and so variable and so L_{it} is the labor force at quinquennial date t.

- *Country capital-emissions ratio*: The capital-emissions ratio H_{it} is constructed from K_t and $\tilde{c}_{it}^{fos}$. Annual data on country capital stock K_{it} comes from the Penn World Tables (PWT) 9.1. We use stocks at quinquennial dates, 1990,1995, etc. We use stocks at quinquennial dates, 1990,1995, etc., and current value PPP in constant 2011 dollars. K_{it} is divided by $\tilde{c}_{it}^{fos}$, five year flow of emissions from country i ending in quinquennial date t. The source for $\tilde{c}_{it}^{fos}$ is given above.

7.5 Output Estimation Details and Robustness Checks

The derivation of the estimating equation in Appendix 7.2 produces the estimating equation (25). Estimation of the reduced production equation is in OLS with country fixed effects, and pooled within each country cluster. The constant is the value of country-fixed dummy. The remaining coefficients can be expressed as $B_{k_s}, \gamma_{k_s}, \zeta_{k_s}$, and η_{k_s} correspond to the cluster k_s in the clustering/partitioning strategy s.

All told, we estimate results for eight clustering strategies: In order they are: (i) Human Development Index (HDI). Here, k ranges over four clusters are High, Medium High, Medium Low, and Low development groups as defined by the World

Table 6: Policy-Adjusted Elasticities by HDI without Capital-Emissions Variable.

	Dependent Variable - Log GDP				
Coefficients	High	Medium High	Medium Low	Low	All
B Carbon Stock	0.767***	0.833***	-0.012	0.055	0.372***
	(0.120)	(0.162)	(0.163)	(0.125)	(0.073)
γ Fossil Fuel	0.126	1.120***	1.065***	0.903***	0.960***
	(0.135)	(0.117)	(0.112)	(0.124)	(0.064)
η Labor Force	0.526***	0.395***	0.684***	0.797***	0.616***
	(0.117)	(0.149)	(0.147)	(0.149)	(0.072)
Observations	184	176	144	132	636
R^2	0.995	0.995	0.996	0.993	0.995
F Statistic	550.4	589.9	644.1	415.7	643.8

Includes Country-Fixed Effects. Standard errors in parentheses. Symbols *, **, and *** indicate statistically significant at the 10%, 5%, and 1% levels, respectively. Based on Human Development Index (HDI), U.N. Development Programme. #Observations = # countries in cluster × 5 quinquennial time periods, 1995-2015.

Bank HDI. (ii) Global sample. There is a single k containing all 152 countries; (iii) Binary HDI - binary partition where k groups High together with Medium High, and Low together with Medium Lowq development. (iv) OECD Membership - binary partition where k ranges over two groupings, OECD countries and all others; (v) Top 30 GDP countries - binary partition where k ranges over "in" and "out" of the top 30; (vi) Top 30 Emitters - binary partition where k ranges over "in" and "out" of the top group; (vii) Top 35 most forested countries - binary partition where k ranges over "in" and "out" of the top group; (viii) Geographic cluster with six groupings: North America (excluding Mexico), Central and South America (including Mexico), Europe, Asia, Oceana, and Africa.

The paper focusses on (i) the HDI and (ii) global cluster. Results for these are reported in Table 2 in Section 4.3. Results of the other six strategies are reported in an external, online appendix. All data, including membership list for each cluster in each of the 8 strategies is available upon request.

In addition, we sought to test for omitted variables by considering alternative specifications that include or exclude key time-trending variables, namely the capital-emissions variable. Table 6 provides estimates for a model that excludes the capital-emissions ratio. Table 7 includes an explicit time trend that substitutes for the capital-emissions variable.

Table 7: Policy-Adjusted Elasticities by HDI, substituting Time Trend for Capital-Emissions variable

	Dependent Variable - Log GDP				
Coefficients	High	Medium High	Medium Low	Low	All
B Carbon Stock	0.157**	0.340***	0.088	0.075	0.092**
	(0.078)	(0.139)	(0.144)	(0.118)	(0.055)
γ Fossil Fuel	0.514***	0.597***	0.845***	0.737***	0.736***
	(0.081)	(0.109)	(0.105)	(0.126)	(0.048)
Time Trend	0.025***	0.030***	0.028***	0.018***	0.028***
	(0.002)	(0.003)	(0.005)	(0.005)	(0.001)
η Labor Force	-0.077	-0.101	-0.014	0.351**	-0.074
	(0.076)	(0.130)	(0.178)	(0.188)	(0.062)
Observations	184	168	136	120	608
R^2	0.998	0.997	0.997	0.994	0.998
F Statistic	1631.5	929.9	815.0	454.3	1213.3

Includes Country-Fixed Effects. Time trend b^t substituting for Capital-emissions ratio H_{it} in Eq. (25). Standard errors in parentheses. Symbols *, **, and *** indicate statistically significant at the 10%, 5%, and 1% levels, respectively. Based on Human Development Index (HDI), U.N. Development Programme. #Observations = # countries in cluster $\times$ 4 lagged quinquennial time periods up to 2015.

7.6 Land Sink Estimation

Restricting attention to the quinquennial periods from 1990 to 2015, a reasonable sample size is obtained by estimating the quinquennial flows *annually* since 1982. The annual 5-year rolling aggregate for global land sink is defined as

$$\tilde{s}_\tau^{lan} = \sum_{j=0}^{4} s_{\tau-j}^{lan} \tag{52}$$

for τ annual. In addition,

$$\widetilde{\rho}_\tau^{lan} = \frac{\tilde{s}_\tau^{lan}}{\omega_{\tau-5}^{lan}} \tag{53}$$

which is assumed identical across countries. In words, $\widetilde{\rho}_\tau^{lan}$ is the quinquennial absorption rate based on the land sink summed over the five year period up to and including annual date τ. We estimate

$$\log(\widetilde{\rho}_\tau + 1) \;=\; \pi_0 + \pi_1 g_{\tau-5} + \pi_2 g_{\tau-5}^2 + \nu_\tau \tag{54}$$

where τ is the standard period length of a year, and we assume $E[\nu_\tau | g_{\tau-5}] = 0$. The equation system is a rolling aggregate of 5 year flows and end-of-period stocks for each period τ where τ varies yearly from 1987-2016, and the data series for all stocks start in 1982.[21]

7.7 Projected Data and Simulation Details

The paths for $\{\tilde{y}_{it}\}$ and $\{\omega_{it}^{lan}\}$ are simulated for $t = 2020, 2025, 2030, \ldots, 2100$ under four RCP scenarios, each corresponding to Global Radiative Forcing levels 2.5, 4.5, 6.0, and 8.5, respectively, in the year 2100.

7.7.1 *Parameter Values from the Model*

Parameter values used in the simulation are the estimated values $\hat{B}$, $\hat{\gamma}$, $\hat{\zeta}$, $\hat{\eta}$, and the fixed-effects constants for countries in a given cluster, and $\hat{\pi}_0$, $\hat{\pi}_1$, and $\hat{\pi}_2$ from the land sink absorption equation.

[21] The rolling aggregate structure induces serial correlation in errors so that OLS will generally be inefficient but unbiased. With additional assumptions on the covariance matrix, (54) can be re-estimated by GLS.

7.7.2 *Projected GHG Series* $\{g_{t,\,RCP}\}$

The source for GHG Series $\{g_{t,\,RCP}\}$ the database for the Representative Concentration Pathways (RCPs) housed at the International Institute for Applied Systems Analysis (IIASA), accessed 2-20-2019. IIASA provides data for the four main RCP scenarios. Each scenario is produced by a distinct modeling group. The RCPs aggregate at the regional/development level, dividing countries according to five categories: the OECD 90 (includes the expanded list of OECD countries, the reforming economies (mostly Eastern Europe), Asia, Middle East and Africa, and Latin America. According the IIASA,

> "The RCPs, which replace and extend the scenarios used in earlier IPCC assessments [prior to AR5], are compatible with the full range of stabilization, mitigation, and baseline emission scenarios available in the current scientific literature."

The model assumptions are outlined as follows.

- RCP 2.6: Stipulates peak radiative forcing at $\approx\ 3W/m^2$ before declining to $2.6W/m^2$ by 2100. RCP 2.6 represents mitigation scenarios with full from all countries to limit the increase of global mean temperature to $2°C$. It forecasts negative energy use emissions growth in the second half of the 21st century due to a low carbon factor (carbon per energy unit), low energy intensity (energy use per dollar income) and low population growth. The economic part assumes that market share of a certain technology or fuel type depends on costs relative to competing technologies. Reference: van Vuuren et al. (2006, 2007).

- RCP 4.5: Stabilizes radiative forcing at $4.5W/m^2$ in 2100 without ever exceeding that value (no overshooting). The economic model is a cost-minimizing policy pathway that reaches the target radiative forcing. The cost-minimizing policy drives changes in the energy system, including shifts to electricity, to lower emissions energy technologies and to the deployment of carbon capture and geologic storage technology. Emissions pricing also applies to land use emissions; as a result, forest lands expand from their present day extent. Reference: Clarke et al. (2007) (Mini-CAM), Smith and Wigley (2006), and Wise et al. (2009).

- RCP 6.0. Stabilizes radiative forcing at $6.0W/m^2$ by 2100, without overshooting. It uses AIM/CGE which models a disaggregated energy system with both

supply and demand sides. The pathway is achieved in a general equilibrium model with non-forward-looking agents, and with technology-explicit modules in power sectors. Source: Fujino et al. (2006) and Hijioka et al. (2008).

- RCP 8.5. Stipulates a rising radiative forcing pathway leading to $8.5W/m^2$ in 2100. RCP 8.5 uses the IAM, MESSAGE and forecasts higher carbon factor, energy intensity, and population growth. The economic model consists of forward looking, representative-agent optimization to obtain consumption, savings, and investment. Source: Riahi and Nakicenovic (2007).

Notes. Various disclaimers on the IIASA site note RCPs are "not new, fully integrated scenarios (i.e., they are not a complete package of socioeconomic, emissions, and climate projections)." and "do not represent specific futures with respect to climate policy action (or no action) or technological, economic, or political viability of specific future pathways or climates." (Characteristics and guidance, IIASA.

7.7.3 *Projected Country Land Carbon Stocks* $\omega^{lan}_{it\,RCP}$

Projected country land carbon stocks from 2020-2100 are constructed from RCP concentrations data, HDI parameter estimates from Table 2, and equilibrium conditions as follows.

Model Calibrated Land Sink Absorption Projections $\widehat{\widetilde{\rho}}_{t,RCP}$ Let

$$\log(\widehat{\widetilde{\rho}}_{t,RCP}+1)=\hat{\pi}_0+\hat{\pi}_1 g_{t-5,RCP}+\hat{\pi}_2 g^2_{t-5,RCP} \tag{55}$$

be the predicted value of the log of the return to land sink absorption under the RCP forecast $\{g_{t,RCP}\}$ and estimates $\hat{\pi}_0$, $\hat{\pi}_1$, and $\hat{\pi}_2$ of the land sink absorption equation.

Calculation of Equilibrium Law of Motion for Land Carbon. Estimate a parameter, in-sample, from the law of motion of land under equilibrium land policy. Combining the land stock law of motion in with equilibrium land use policies, one obtains

$$\begin{aligned}\omega^{lan}_{it} &= \omega^{lan}_{it-5}-\tilde{c}^{*lan}_{it}(\omega^{lan}_{it-5})+\tilde{r}^{*lan}_{it}(\omega^{lan}_{it-5})+\tilde{s}^{lan}_{it}\\ &= D_i\left(2\omega^{lan}_{i\,t-5}+\tilde{s}^{lan}_{it}\right)\\ &= D_i\omega^{lan}_{i\,t-5}\left(2+\widetilde{\rho}_t\right)\end{aligned} \tag{56}$$

where $D_i\equiv 1-\frac{(1-\delta)(\alpha_i+\theta_i)}{\alpha_i+\beta_i+\theta_i}$ is the model-generated adjustment factor. This is independent of t. Equation (56) describes the theoretical carbon stock dynamics under equilibrium land use. The evolution of ω^{lan}_{it} depends on the land carbon adjustment

factor D_i derived from land use. The *empirical adjustment factor* D_{it} from sample data is

$$D_{it} \equiv \frac{\omega_{it}^{lan}}{\omega_{i\,t-5}^{lan}\left(2+\widehat{\widetilde{\rho}}_t\right)}. \tag{57}$$

which, unlike the model generated parameter, will generally depend on t due to shocks.

Now, average these empirical adjustment factor over four time periods, 2000, 2005, 2010, 2015, and over all countries in a given cluster k, using HDI as our partition. Thus *average adjustment factor* D_k cluster k is computed as:

$$D_k \equiv \frac{1}{4 \times \#\{\text{ i in cluster } k\ \}} \sum_{t\in 2000}^{2015} \sum_{i\in \text{cluster } k} D_{it} \tag{58}$$

The computations of these average adjustment factors across HDI clusters are displayed in Table 8.

Table 8: Mean Adjustment Factors under equilibrium Land Policies.

	High HDI	Med High HDI	Med Low HDI	Low HDI
Adjustment Factor D_k	0.5196	0.5062	0.4816	0.4727
	(0.0477)	(0.0604)	(0.0368)	(0.0598)

Standard deviations (not standard errors) in parentheses.

Equation for Projected Land Stocks. Generate the RCP forecasted series $\{\omega_{it,RCP}^{lan}\}$ recursively using the equation

$$\omega_{it,RCP}^{lan} = D_k \omega_{it-5,RCP}^{lan}[2+\widehat{\widetilde{\rho}}_{t,RCP}] \tag{59}$$

for country i in cluster k under scenario RCP starting from $t-5=2015$, with each t representing a quinquennial time period.

7.7.4 *Projected Country Fossil Fuel Emissions* $\tilde{c}_{it,\,RCP}^{fos}$

There are four distinct series each based in one of the four RCPs (see sources for each RCP). The construction of $\tilde{c}_{it,\,RCP}^{fos}$ is done by estimating the decadal percentage

variation of GHG emissions, excluding LUCF, for each region in each RCP. These growth rates are then attributed to each country within that region. To account for the different GHGs we convert each gas into CO2e units using standard conversion factors from global warming potential as specified in the IPCC 5th Assessment Report.

The equation below for the change Δ in fossil fuel emissions describes which gases are included. For region j we define

$$\Delta_{j,t,RCP} = \text{CO2 fossil fuel}_{j,t,RCP} + \left(\text{total CH4} - \underbrace{(\text{CH4 from grassland and forest burn})}_{\text{LUCF}} \right)_{j,t,RCP} + \text{other GHGs}_{j,t,RCP} \tag{60}$$

where all emissions are in CO2e.

Then the $\tilde{c}^{fos}_{ijt,RCP}$ of the country i that belong to the region j under the RCP, when $t \in \{2020, 2030, 2040, \ldots, 2100\}$ is given by:

$$\tilde{c}^{fos}_{i,j,t+10,RCP} = \tilde{c}^{fos}_{ijt,RCP} \frac{\Delta_{j,t+10,RCP} - \Delta_{j,t,RCP}}{\Delta_{j,t,RCP}}$$

Then for mid-decade dates $t \in \{2025, 2035, 2045, \ldots, 2095\}$ the projection for fossil fuel is given by:

$$\tilde{c}^{fos}_{it,RCP} \;=\; \frac{1}{2}\tilde{c}^{fos}_{i\,t-5,\,RCP} \;+\; \frac{1}{2}\tilde{c}^{fos}_{it+5,RCP}.$$

7.7.5 *Projected Country Capital-emissions ratios* $H_{it,\,RCP}$

We construct a forecasted series $\{H_{it,\,RCP}\}$, for $t = 2020, 20205, \ldots, 2100$ across the four RCP scenarios. Dropping the RCP designation in the notation, we construct paths assuming a fixed quinquennial rate of improvement,

$$H_{i\,t+1} \;=\; (1+h)H_{it} \tag{61}$$

We impute a value of h that will vary across the four RCPs. The variable h will be imputed from RCP assumptions.

Decomposition and Kaya Identity. The decomposition of H_{it} is

$$H_{it} \;=\; \frac{K_{it}}{c_{it}^{fos}} \;=\; \frac{K_{it}}{E_{it}} \times \frac{E_{it}}{c_{it}^{fos}} \tag{62}$$

where E_{it} is the total energy usage (in GJ units) by country i during quinquennial time period up to and including date t.

Define z_k, z_f by

$$\begin{array}{rcl} \dfrac{K_{i\,t+1}}{E_{i\,t+1}} & = & (1+z_k)\dfrac{K_{it}}{E_{it}} \\ \dfrac{E_{i\,t+1}}{c_{i\,t+1}^{fos}} & = & (1+z_f)\dfrac{E_{it}}{c_{it}^{fos}}. \end{array} \tag{63}$$

We obtain

$$(1+h) \;=\; (1+z_k)(1+z_f) \tag{64}$$

To complete the construction, we derive values of z_k and z_f from the RCP assumptions. RCPs make assumptions using the *Kaya Identity*,

$$c_{it}^{fos} \;=\; L_{it} \times \underbrace{\frac{y_{it}}{L_{it}}}_{\text{per capita GDP}} \times \underbrace{\frac{E_{it}}{y_{it}}}_{\text{energy intensity}} \times \underbrace{\frac{c_{it}^{fos}}{E_{it}}}_{\text{carbon factor}}$$

Each RCP makes assumptions about projected energy intensity (EI) $\frac{E_{it}}{y_{it}}$, and carbon factor (CF) $\frac{c_{it}^{fos}}{E_{it}}$. Notice that the second equation in (63) describes the evolution of the *inverse carbon factor (ICF)*, $\frac{E_{it}}{c_{it}^{fos}}$.

Calibrated Values. Now let x_e and x_f denote the proportional reductions in EI and CF, respectively, over a quinquennial (5yr) time period. Formally, these are defined by

$$\begin{array}{rcl} \dfrac{E_{i\,t+1}}{y_{i\,t+1}} & = & (1-x_e)\dfrac{E_{it}}{y_{it}} \\ \dfrac{c_{i\,t+1}^{fos}}{E_{i\,t+1}} & = & (1-x_f)\dfrac{c_{it}^{fos}}{E_{it}} \end{array} \tag{65}$$

for quinquennial dates t, where flows are five year sums. We approximate the average quinquennial improvements x_e and x_f assumed in each RCP from van Vuuren (2011,

Table 9: Rate Reductions in IE and CF

	Rate x_e of reduction in IE (5 yr)	Rate x_f of reduction in CF (5yr)
RCP 2.6	0.0670	0.1684
RCP 4.5	0.0635	0.0620
RCP 6.0	0.0607	0.0059
RCP 8.5	0.0107	0.0081

Table 10: Rate Increase in ICF over all RCPs

	Rate z_f of increase in ICF (5yr)
RCP 2.6	0.2025
RCP 4.5	0.0661
RCP 6.0	0.0059
RCP 8.5	0.0082

Fig. 7). The values are reported in Table 9. The values in Table 9 are found by computing the % change over each quinquennial period needed to obtain the net change over the entire period from 2000 to 2100 as described in van Vuuren (2011).[22]

Note a proportional decrease of x_f in the carbon factor corresponds to a proportional increase $z_f = \frac{x_f}{1-x_f}$ in the inverse carbon factor. This formula is utilizes the values in Table 9 to produce Table 10.

The remaining task is to find/approximate z_k. Using the definitions in (63) and (65) we obtain

$$\begin{aligned}
\frac{\frac{K_{i\,t+1}-K_{it}}{K_{it}}}{\frac{E_{i\,t+1}-E_{it}}{E_{it}}} &= 1 + z_k \frac{E_{i\,t+1}}{E_{i\,t+1}-E_{it}}, \text{ and} \\
\frac{\frac{c^{fos}_{i\,t+1}-c^{fos}_{it}}{c^{fos}_{it}}}{\frac{E_{i\,t+1}-E_{it}}{E_{it}}} &= 1 - x_f \frac{E_{i\,t+1}}{E_{i\,t+1}-E_{it}} \qquad (66) \\
\frac{\frac{y_{i\,t+1}-y_{it}}{y_{it}}}{\frac{E_{i\,t+1}-E_{it}}{E_{it}}} &= 1 + z_e \frac{E_{i\,t+1}}{E_{i\,t+1}-E_{it}}
\end{aligned}$$

where $z_e = x_e/(1-x_e)$ is the proportional increase in inverse energy intensity $\frac{y_{it}}{E_{it}}$.

Taking the log of our initial output equation and differentiating with respect to

[22]See Riahi (2011) for alternative forecasts of CF and IE.

E_{it} we obtain an instantaneous elasticity decomposition,

$$\frac{E_{it}\partial y_{it}}{y_{it}\partial E_{it}} \;=\; \zeta_i \left(\frac{E_{it}\partial K_{it}}{K_{it}\partial E_{it}} - \frac{E_{it}\partial c_{it}^{fos}}{c_{it}^{fos}\partial E_{it}} \right) \;+\; \gamma_i \frac{E_{it}\partial c_{it}^{fos}}{c_{it}^{fos}\partial E_{it}} \tag{67}$$

The instantaneous elasticities in (67) approximate the discrete elasticities, i.e.,

$$\frac{E_{it}\partial K_{it}}{K_{it}\partial E_{it}} \approx \frac{\frac{K_{i\,t+1}-K_{it}}{K_{it}}}{\frac{E_{i\,t+1}-E_{it}}{E_{it}}},$$

$$\frac{E_{it}\partial c_{it}^{fos}}{c_{it}^{fos}\partial E_{it}} \approx \frac{\frac{c_{i\,t+1}^{foss}-c_{it}^{foss}}{c_{it}^{foss}}}{\frac{E_{i\,t+1}-E_{it}}{E_{it}}}$$

and

$$\frac{E_{it}\partial y_{it}}{y_{it}\partial E_{it}} \approx \frac{\frac{y_{i\,t+1}-y_{it}}{y_{it}}}{\frac{E_{i\,t+1}-E_{it}}{E_{it}}}$$

Using these approximations, we substitute the discrete elasticities in (66) into the instantaneous elasticity decomposition (67) to obtain

$$1+z_e\frac{E_{i\,t+1}}{E_{i\,t+1}-E_{it}} \;=\; \zeta_i \left(z_k \frac{E_{i\,t+1}}{E_{i\,t+1}-E_{it}} + x_f \frac{E_{i\,t+1}}{E_{i\,t+1}-E_{it}} \right) + \gamma_i \left(1 - x_f \frac{E_{i\,t+1}}{E_{i\,t+1}-E_{it}} \right)$$

Solving for z_k we obtain,

$$z_k \;=\; (1-\gamma_i)\frac{E_{i\,t+1}-E_{it}}{E_{i\,t+1}} + \frac{z_e}{\zeta_i} + \frac{(\gamma_i-\zeta_i)x_f}{\zeta_i} \tag{68}$$

Rewriting this equation,

$$z_k \;=\; (1-\gamma_i)\left(\frac{E_{i\,t+1}-E_{it}}{E_{i\,t+1}} - x_f \right) + \frac{z_e}{\zeta_i} + \frac{(1-\zeta_i)x_f}{\zeta_i} \tag{69}$$

For γ_i close to one and/or $\frac{E_{i\,t+1}-E_{it}}{E_{i\,t+1}}$ close to x_f, we obtain

$$z_k \;\approx\; \frac{z_e}{\zeta_i} + \frac{(1-\zeta_i)x_f}{\zeta_i} \tag{70}$$

Our estimates for γ_i are $0.769, 1.083, 1.103, 0.861$ for High, Med High, Med Low and Low Human Development clusters, resp. Our global estimate of γ is 0.992. All are significant at 1% level. Thus, using the approximation in (70) with our estimates for ζ_i across HDI clusters, we obtain

Approximate rate z_k of increase in K_{it}/c_{it}^{fos}

RCP/cluster	H	MH	ML	L
RCP 2.6	0.5090	1.6520	1.1359	1.2121
RCP 4.5	0.3040	0.9219	0.6428	0.6840
RCP 6.0	0.1930	0.5287	0.3770	0.3994
RCP 8.5	0.0638	0.1852	0.1304	0.1384

Table 3

Now use the values of Table 2 and Table 3 in order to compute h from equation (64). Finally, we can compute the series $\{\tilde{H}_{it,\,RCP}\}$ from equation (61).

7.7.6 *Projected Country Labor* L_{it}

This section describes how 2020-2100 country labor force projections are constructed from population and labor force participation forecasts. Source data for population forecasts from U.N. World Population Prospects 2019. Source data for particpation rates come from the World Bank, World Development Indicators (see online appendix).

Steps for constructing projected labor series. Projected labor force projection by country at quinquennial date t in the time period 2020-2100 is given by:

(Country population in year t) $\times$ (participation rate in corresponding year t).

We will be precise about how these are calculated.

First, projected population data is described in point (i) above. To be consistent with labor participation data, population is aggregated into 4 age/sex categories, Male 15-54, Male 65+, Female 15-64, Female 65+. In the formulae below, Pop_{ita} will denote the population of country i at quinquennial date t restricted to the age/sex category a, where

$$a \in \{ \text{ Male 15-54, Male 65+, Female 15-64, Female 65+ } \}.$$

Second, projected participation rates are constructed as follows in the following steps.

1. Each country is classified into one of five categories: High income developed (HID), High income emerging (HIE), upper middle income (UMI), lower middle income (LMI), low income (LI).

2. The average participation rate of High income developed (HID) countries is assumed to remain stationary after 2020. It remains at its 2020 average rate.

3. With one caveat, each country in each classification is assumed to converge to the stationary average HID rate. The date of convergence depends on classification. HID countries of course converge to the HID average in 2020. HIE countries and UMI countries converge in 2040. LMI countries converge in 2070. LI converge in 2100.

4. The caveat: any country with participation rate *below* the average HID rate in 2020 remains stationary at its 2020 rate. Participation rates thus fall in income/development.

5. Until its date of convergence, each country's participation rate at quinquennial date t is calculated as a linear interpolation between 2017 and its convergence date. More precisely, the formula is as follows: Let y_g be the year of converge of a country in income g. Let $\bar{PR}_a$ denote the average participation rate of age/sex group a across HID countries in the year 2020 (the stationary rate). Then, the participation rate PR_{ita} for members of age/sex group a of country i in group g at quinquennial date t such that $2017 < t < y_g$ is

$$PR_{ita} \;=\; P_{i,\,2017,\,a} \;+\; (\bar{PR}_a \;-\; P_{i,\,2017,\,a}) \times \frac{t - 2017}{y_g - 2017}$$

6. Finally, we calculate labor force L_{it} of country i at quinquennial date t as

$$L_{it} \;=\; \sum_a PR_{ita} \times Pop_{ita}$$